

ISSN 2457 - 5275 (Online, English)
ISSN 1842 - 4074 (Print, Online, Romanian)

June 2019
Volume 25
Number 2
4th Series

RoJAE

Romanian Journal of Automotive Engineering

SIAR

The Journal of the Society of Automotive Engineers of Romania
www.siar.ro
www.ro-jae.ro

RoJAE Romanian Journal of Automotive Engineering

SIAR

Societatea Inginerilor de Automobile din România
Society of Automotive Engineers of Romania
www.siar.ro

SIAR – The Society of Automotive Engineers of Romania is the professional organization of automotive engineers, an independent legal entity, non-profit, active member of FISITA (Fédération Internationale des Sociétés d'Ingénieurs des Techniques de l'Automobile - International Federation of Automotive Engineering Societies) and EAEC (European Cooperation Automotive Engineers).

Founded in January 1990 as a professional association, non-governmental, SIAR's main objectives are: development and increase the exchange of professional information, promoting Romanian scientific research results, new technologies specific to automotive industry, international cooperation.

Shortly after its constitution, SIAR was affiliated to FISITA - International Federation of Automotive Engineers and EAEC - European Conference of Automotive Engineers, thus ensuring full involvement in specific activities undertaken globally.

In order to help promoting the science and technology in the automotive industry, SIAR is issuing 4 times a year rIA - Journal of Automotive Engineers (on paper in Romanian and electronically in Romanian and English).

The organization of national and international scientific meetings with a large participation of experts from universities and research institutes and economic environment is an important part of SIAR's. In this direction, SIAR holds an annual scientific event with a wide international participation. The SIAR annual congress is hosted successively by large universities that have ongoing programs of study in automotive engineering.

Developing relationships with the economic environment is a constant concern. The presence in Romania of OEMs and their suppliers enables continuous communication between industry and academia.

Actually, a constant priority in SIAR's activity is to ensure optimal framework for collaboration between universities and research, industry and business specialists.

The Society of Automotive Engineers of Romania

President

Adrian-Constantin CLENCI
University of Pitesti, Romania

Honorary President

Eugen Mihai NEGRUS
University „Politehnica” of Bucharest, Romania

Vice-Presidents

Cristian-Nicolae ANDREESCU
University „Politehnica” of Bucharest, Romania

Nicolae BURNETE
Technical University of Cluj-Napoca, Romania

Victor CEBAN
Technical University of Moldova, Chisinau, Moldova

Anghel CHIRU
„Transilvania” University of Brasov, Romania

Liviu-Nicolae MIHON
Politehnica University of Timisoara, Romania

Victor OTAT
University of Craiova, Romania

Ion TABACU
University of Pitesti, Romania

General Secretary

Minu MITREA
Military Technical Academy of Bucharest, Romania

Honorary Committee of SIAR

Alexander SIMIONESCU

Renault Technologie Roumanie
www.renault-technologie-roumanie.com

Benone COSTEA

Magic Engineering srl
<http://www.magic-engineering.ro>

George-Adrian DINCA

Romanian Automotive Register
www.rarom.ro

Radu DINESCU

The National Union of Road Hauliers from Romania
www.untrr.ro

Gerolf STROHMEIER

AVL Romania
www.avl.com



SIAR – Society of Automotive Engineers of Romania is member of:



FISITA - International Federation of Automotive Engineers Societies
www.fisita.com

EAEC - European Automotive Engineers Cooperation



CONTENTS

Volume 25, Issue No. 2

June 2019

| | |
|--|----|
| Comparative Analysis of the Cyclist Safety Performances Yielded by External and Helmet Airbags Ovidiu Andrei CONDREA, Anghel CHIRU, George TOGĂNEL and Daniel Dragoș TRUȘCĂ | 41 |
| The NEPCM Material as Cooling Solutions for High Power Light Emitting Diodes (LED) Dorin LELEA and Adrian Eugen CIOABLĂ | 49 |
| Efficiency Analysis of Passive Safety Systems in Vehicles in the Case of Frontal Collision Using Experimental Tests Alexandru Ionut RADU, Daniel Dragoș TRUȘCĂ, George TOGANEL and Bogdan TOLEA | 55 |
| Design Optimization of a Passenger Car's Steering System for Minimizing the Ackerman Error and the Turning Radius Augustin CONSTANTINESCU, Mario TROTEA, Loreta SIMNICEANU and Gheorghe POPA – MITROI | 65 |

The RoJAE's articles are included in the „*Ingineria automobilului*” magazine (ISSN 1842 – 4074), published by SIAR in Romanian.

The articles published in „*Ingineria automobilului*” magazine are indexed by Web of Science in the „*Emerging Source Citation Index (ESCI)*” Section.

Web of Science



RoJAE 25(2) 37 – 72 (2019)

ISSN 2457 – 5275 (Online, English)

ISSN 1842 – 4074 (Print, Online, Romanian)

The journals of SIAR are available at the website www.ro-jae.ro.

RoJAE

Romanian

Journal of Automotive Engineering

Editor in Chief

Cornel STAN

West Saxon University of Zwickau, Germany

E-mail: cornel.stan@fh-zwickau.de

Technical and Production Editor

Minu MITREA

Military Technical Academy, Bucharest, Romania

E-mail: minumitrea@yahoo.com

Contributors

Adrian Eugen CIOABLĂ

Anghel CHIRU

Ovidiu – Andrei CONDREA

Augustin CONSTANTINESCU

Dorin LELEA

Gheorghe POPA-MITROI

Alexandru Ionuț RADU

Loreta SIMNICEANU

George TOGĂNEL

Mario TROTEA

Daniel Dragoș TRUȘCĂ

Bogdan ȚOLEA

The authors declare that the material being presented in the papers is original work, and does not contain or include material taken from other copyrighted sources.

Wherever such material has been included, it has been clearly indented or/and identified by quotation marks and due and proper acknowledgements given by citing the source at appropriate places. The views expressed in the articles are those of the authors and are not necessarily endorsed by the publisher.

While every case has been taken during production, the publisher does not accept any liability for errors that may have occurred.

Advisory Editorial Board

Dennis ASSANIS

University of Michigan, USA

Rodica A. BARANESCU

Chicago College of Engineering, USA

Michael BUTSCH

University of Applied Sciences, Konstanz, Germany

Nicolae BURNETE

Technical University of Cluj-Napoca, Romania

Giovanni CIPOLLA

Politecnico di Torino, Italy

Felice E. CORCIONE

Engines Institute of Naples, Italy

Georges DESCOMBES

Conservatoire National des Arts et Metiers de Paris, France

Cedomir DUBOKA

University of Belgrade, Serbia

Pedro ESTEBAN

Institute for Applied Automotive Research Tarragona, Spain

Radu GAIGINSCHI

„Gheorghe Asachi” Technical University of Iasi, Romania

Eduard GOLOVATAI-SCHMIDT

Schaeffler AG & Co. KG Herzogenaurach, Germany

Ioan-Mircea OPREAN

University „Politehnica” of Bucharest, Romania

Nicolae V. ORLANDEA

University of Michigan, USA

Victor OTAT

University of Craiova, Romania

Andreas SEELINGER

Institute of Mining and Metallurgical Engineering, Aachen, Germany

Ulrich SPICHER

Karlsruhe University, Karlsruhe, Germany

Cornel STAN

West Saxon University of Zwickau, Germany

Dinu TARAZA

Wayne State University, USA

SIAR

The Journal of the Society of Automotive Engineers of Romania

www.ro-jae.ro

www.siar.ro

Copyright © SIAR

Production office:

The Society of Automotive Engineers of Romania (Societatea Inginerilor de Automobile din România)

Facultatea de Transporturi, Splaiul Independentei Nr. 313

060042 Bucharest ROMANIA Tel.: +4.021.316.96.08 Fax: +4.021.316.96.08 E-mail: siar@siar.ro

Staff: Professor Minu MITREA, General Secretary of SIAR

Subscriptions: Published quarterly. Individual subscription should be ordered to the Production office.

Annual subscription rate can be found at SIAR website <http://www.siar.ro>.

COMPARATIVE ANALYSIS OF THE CYCLIST SAFETY PERFORMANCES YIELDED BY EXTERNAL AND HELMET AIRBAGS

Ovidiu Andrei CONDREA^{*}, Anghel CHIRU, George TOGĂNEL, Daniel Dragoș TRUȘCĂ

Transilvania University of Brașov, Str. Politehnicii Nr. 1, 500024 BRASOV, Romania

(Received 14 March 2019; Revised 31 March 2019; Accepted 2 May 2019)

Abstract: This study investigates in an experimental approach the passive safety performances of the most recent airbag technologies for cyclists: helmet airbags and vehicle-mounted external airbags. Two staged tests were performed under similar initial conditions and using the same vehicle: Test 1 (10.4 m/s vehicle impact velocity, dummy equipped with helmet airbag) and Test 2 (11.1 m/s vehicle impact velocity, vehicle equipped with external airbag). The performances of the passive safety systems are assessed by comparing the measured linear accelerations, HIC and NIC values, while also addressing the time of airbag deployment. Results show that helmet airbags offer higher protection in terms of injury reduction, but the deployment time is significantly higher than for external airbags. In the case of external airbags however, a significant potential in mitigating head injuries was identified, yet additional research is required in order to optimize airbag volume, inclination and deployment time.

Key-Words: *Helmet airbag. External airbag. Cyclist airbag. Cyclist safety. Cyclist impact. Safety performance*

NOMENCLATURE

HIC : head injury criterion

NIC : neck injury criterion, m^2/s^2

a : resultant head acceleration, m/s^2

a_x^{T1} : T1 vertebra acceleration measured on the X axis, m/s^2

a_x^H : head acceleration measured on the X axis, m/s^2

a_{rel} : relative acceleration between head and T1 vertebra, m/s^2

v_{rel} : relative velocity between head and T1 vertebra, m/s

1. INTRODUCTION

Cyclists are the most vulnerable road users (VRU) after pedestrians, making cyclist safety an important concern among accidentologists. In 2010, 7.4% of EU road users acknowledged the bicycle as the main mode of transport [5]. During the 2012-2015 period, cyclist fatalities in EU made for 8% of all road fatalities, marking an increase comparing to the 7% rate recorded during the 2009-2011 period [6]. Maki [11] showed that 72% of cyclist fatalities and 21% of cyclist serious injuries are caused by head injuries. Similar findings by Otte [15] show that the frequency of AIS2+ head injuries is 26.7%. These studies offer a clear indicator that head injuries are the leading cause in cyclist fatalities, while also underlining the need for an increased level of protection for cyclists in order to mitigate traumatic brain injuries.

Regarding cyclist head safety, traditional bicycle helmets made from expanded polystyrene represent the most widespread passive safety equipment for cyclists, and their role in reducing linear and angular accelerations, as well as impact forces, has been acknowledged in a series of studies [2][3][12][13][16][19]. However, new passive safety systems for cyclists have been developed in recent years by innovating airbag technologies, namely helmet airbags for cyclists and vehicle-mounted external airbags which are designed to improve the safety of pedestrians and other VRU.

To this point, the cyclist safety potential of these airbag systems is not comprehensively determined.

^{*} Corresponding author e-mail: ovidiu.condrea@unitbv.ro

It has been shown through vertical and oblique drop tests [10][18] that helmet airbags perform better than traditional bicycle helmets, significantly reducing HIC values (to a maximum of 7-8 times if optimized) [10] and linear acceleration (nearly three times) [18].

Furthermore, helmet airbags reduced rotational acceleration values minimum three times compared to MIPS helmets in most of the cases [18], which is notable taking into account that the latter are specifically designed to limit the angular acceleration of the head in comparison with conventional bicycle helmets. However, there is a need for further evaluation of helmet airbags [10] since there is no information in literature about the performance of helmet airbags in full-scale staged tests, therefore the potential of these types of safety systems in realistic vehicle-bicycle accident scenarios is still undetermined.

Vehicle external airbags have been developed in recent years and integrated into advanced passive safety systems which include active bonnet systems. Kietlinsky [9] showed that the stand-alone performance of external airbags can be summarized in a 30 to 40% reduction in VRU injury values and an 80% reduction if coupled with autonomous emergency braking systems. Similar results were obtained by Frederiksson [7] for pedestrian AIS3+ injury reduction (48%). In a TNO study [17] it was shown that optimized external airbags can reduce HIC values for cyclists by more than 75%, if gas temperature and mass flow are increased. However, the safety potential of external airbags is influenced by vehicle geometry and they are less effective for larger vehicles (SUV, minivans, heavy vehicles) [9]. Furthermore, there are still numerous concerns regarding the de facto cyclist safety provided by external airbags and their optimization for this purpose, since the primary focus for assessing the safety performances of these types of systems was set on the pedestrian category.

The first aim of this paper is to experimentally determine the passive safety performances of helmet airbags and external airbags in cyclist HIC and NIC reduction, thus investigating the proof of concept for these systems. The second aim is to compare the inflation performances of these technical solutions and to determine which one has a higher potential in mitigating cyclist injuries.

2. THE WORKING PRINCIPLE OF EXTERNAL AND HELMET AIRBAGS

2.1 Helmet airbags

Helmet airbags are designed [1][14] to be worn on the neck similar to a scarf and comprise a lower airbag part, an upper airbag part, an inflator, a trigger and an external apparel. The two airbags are initially folded inside the apparel and connected to the inflator, which comprises a hybrid gas generator, a 3 Volt battery and a deflator. The trigger device is manually activated and comprises a micro sensor and auxiliary electronics which control the inflation conditions and prevent false positives. The deployment occurs after the acceleration on the X or Y axes reaches a certain threshold, while the accelerations measured on the Z axis are not taken into account for deployment. This feature was implemented by the manufacturer in order to prevent the deployment of the airbag in non-dangerous situations, such as running over potholes. Upon triggering, the lower airbag inflates first and surrounds the neck and the back of the head, while the upper airbag inflates afterwards and surrounds the crown of the skull, the temporal lobes and the forehead.

2.2 External airbags

External airbags are positioned below the common edge of the vehicle's windscreen and bonnet and are designed to function in tandem with active hood systems, which decrease the rigidity of the bonnet in the proximity of the cowl and create space for airbag deployment. A contact sensor comprised of several accelerometers triggers the deployment after detecting a frontal bumper impact. Deployed external airbags take a U-shape and surround the lower-part of the windscreen and the A-pillars, in this way covering the stiffer areas which cause VRU injuries in impacts. Different versions of external airbags are available, the primary difference being the airbag volume and implicitly the area covered by the airbags. Consequently, external airbags can be pedestrian-only dedicated or VRU dedicated, the latter covering a wider area of the A-pillars.

None of the current external airbag technologies offer protection against head impacts with the roof edge or the upper part of the windscreen, which are generated at higher WAD (wrap-around distance) values, as it is the case for most of the vehicle-bicycle accidents.

3. METHODS

For this study two different experiments were carried out at approximately the same vehicle impact speed in order to allow comparability between helmet and external airbags in terms of injury probability reduction. An Opel Corsa vehicle, two bicycles and a dummy with anthropometric characteristics were used in the experiments. The dummy was instrumented with two tri-axial accelerometers mounted in the centers of mass of the head and the thorax.

In Test 1, the cyclist dummy was equipped with an undeployed helmet airbag, which was manually activated before the test. The airbag inflated before the head impact with the vehicle and maintained a part of the initial air pressure during the head impact with the ground.

In Test 2, the vehicle was equipped with a pedestrian dedicated external airbag connected to an improvised impact sensor comprised of an electrical contact positioned in the vehicle's bumper, in the predicted contact area with the bicycle. The external airbag positioning on the vehicle was carried out inversely in an innovative manner by attaching the airbag to the roof of the vehicle, such that the airbag will cover the frontal edge of the roof upon inflation, the extremity of the windscreen and the upper parts of the A-pillars.

Each crash-test was broken down into four distinct moments (figure 1) which mark the definitory phases of the collision and the phases of the cyclist's kinematic motion:

- The vehicle-bicycle impact (t_0)
- The vehicle-pelvis impact (t_1)
- The vehicle-head impact (t_2)
- Launch-off moment (t_3)

The initial impact between the vehicle and the bicycle was chosen as the starting point for our analysis ($t_0=0$, figure 1.a.).









| Phases of impact | Test 1 | Test 2 |
|--|---|--|
| a) Vehicle-bicycle impact t_0 |  0 ms |  0 ms |
| b) Vehicle - dummy pelvis impact t_1 |  182 ms |  93 ms |
| c) Vehicle - dummy head impact t_2 |  295 ms |  218 ms |
| d) Launch-off moment t_3 |  932 ms |  887 ms |

Figure 1. Film sequences from the carried-out crash-tests

The acquired head and thorax accelerations were processed with a CFC 60 filter and used as input parameters to calculate HIC and NIC criteria values.

HIC was first proposed in 1972 by NHTSA, in the present being one of the most used head injury criteria. The input parameter used to assess HIC values is the resultant head acceleration. Initially, the selected time interval used for HIC calculation was limited to maximum 36 ms (HIC 36), yet in 2000 it was decreased by NHTSA to 15 ms (HIC 15).

$$HIC = \left\{ \left[\frac{1}{t_2 - t_1} \int_{t_1}^{t_2} a(t) dt \right]^{2.5} (t_2 - t_1) \right\}_{\max} \quad (1)$$

NIC was introduced in 1996 and it is currently used to evaluate neck injury probability by using head and T1 vertebra accelerations and velocities as input parameters.

The selected time interval is comprised of 150 ms for which the maximum NIC value is determined.

$$NIC = 0.2 \cdot a_{rel} + v_{rel}^2 \quad (2)$$

$$a_{rel} = a_x^{T1} - a_x^H \quad (3)$$

$$v_{rel} = \int a_{rel} dt \quad (4)$$

For this study, in order to determine NIC values, the T1 vertebra acceleration was assimilated with the acceleration measured in the center of gravity of the dummy's thorax.

4. RESULTS AND DISCUSSION

Vehicle impact velocity was determined as follows: 10.4 m/s for Test 1 and 11.1 m/s for Test 2.

The head impact location was approximately in the same area for both tests, in the superior edge of the windscreen respectively (figure 1. c, figure 2).

The wrap-around distance measured onto the vehicle's frontal profile from ground level to the head impact location, suffered a variation of 30 mm.

The similar head impact location and vehicle impact velocity obtained for each test constituted prerequisites for allowing the comparative analysis to be carried out.



Figure 2. Cyclist head impact location for each crash-test

Head and thorax accelerations acquired during the crash-tests were processed and used for assessing injury criteria values.

The resultant cyclist head and thorax accelerations are shown in figures 3 and 4. Calculated HIC and NIC values, as well as the measured data afferent to each crash-test are presented in Table 1.

The maximum head acceleration was nearly equal for both tests, 86.9 m/s² for Test 1 and 85.8 m/s² for Test 2.

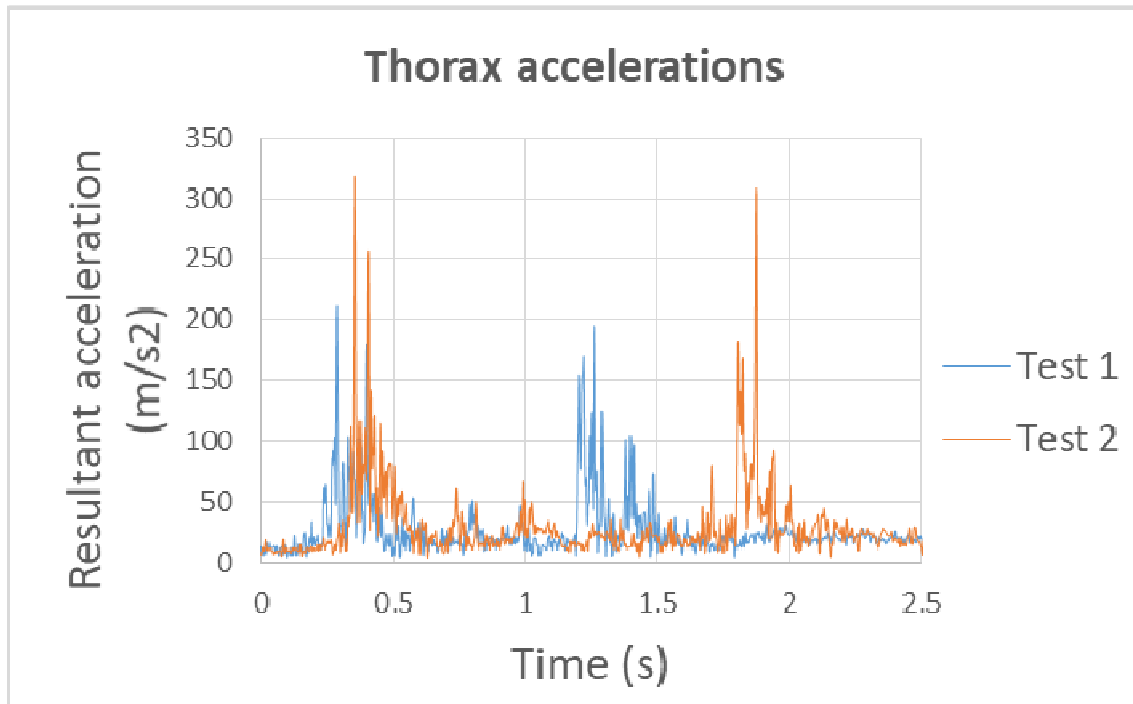


Figure 3. Cyclist thorax accelerations acquired during the crash-tests

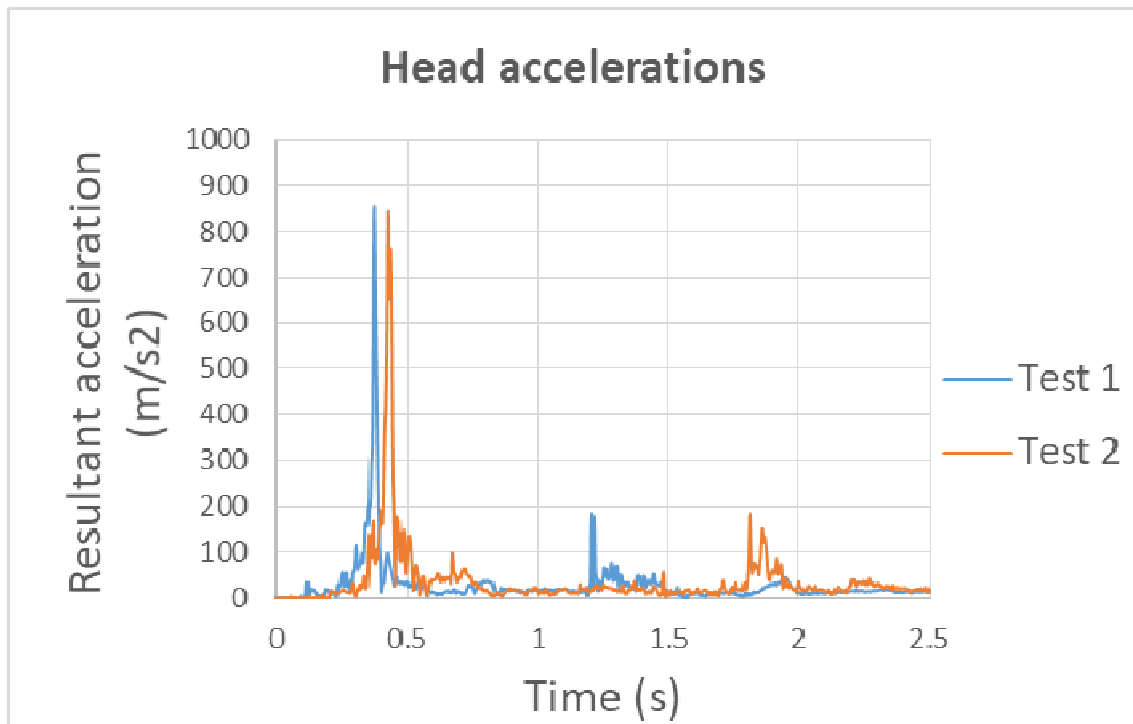


Figure 4. Cyclist head accelerations acquired during the crash-tests

Table 1
 Injury criteria values and measured data afferent to each crash-test

| Test no. | Vehicle impact velocity [m/s] | Pelvis impact time [ms] | Head impact time [ms] | WAD [mm] | Maximum head acceleration [m/s ²] | HIC 15 | HIC 36 | NIC [m ² /s ²] |
|----------|-------------------------------|-------------------------|-----------------------|----------|---|--------|--------|---------------------------------------|
| 1 | 10.4 | 172 | 295 | 2220 | 86.9 | 268 | 167 | 41 |
| 2 | 11.1 | 92 | 218 | 2250 | 85.8 | 498 | 325 | 61 |

Regarding the injury reduction offered by each type of airbag, the helmet airbag decreased the HIC 15 and HIC 36 values with 46% and the NIC value with 32% compared to the external airbag.

For both crash-tests, NIC values exceeded the 15 m²/s² threshold which constitutes the AIS-1 cervical injury tolerance, yet the HIC values did not exceed the threshold of 700 for neither test.

As for the airbags' inflation performance shown in Table 2, significant differences were determined within the video analysis procedure step.

The deployment duration of the external airbag was approximately 20 ms, nearly half of the duration of the helmet airbag – 39 ms respectively.

The start of the external airbag deployment was observed at 93 ms when the cyclist pelvis impact took place, and ended at 113 ms, respectively with 105 ms before the head impact took place.

The debut of the helmet airbag deployment (263 ms) occurred after the pelvis impact.

The deployment process ended at 302 ms, after the head impact took place.

Table 2
 Airbag performance parameters

| Airbag performance parameters | | | | | | |
|-------------------------------|-----------------|-----------------------|-----------------------------------|------------------------------------|---------------------------------|---------------------|
| Test no. | Type of airbag | Head impact time (ms) | Airbag deployment debut time (ms) | End of airbag deployment time (ms) | Airbag deployment duration (ms) | Time to impact (ms) |
| 1 | Helmet airbag | 295 | 263 | 302 | 39 | -39 |
| 2 | External airbag | 218 | 93 | 113 | 20 | 123 |

The external airbag behaved better than the helmet airbag which was not deployed entirely at the time of the head impact.

This is caused by the different types of inflation procedures for each airbag: the external airbag is deployed after the vehicle-bicycle impact is detected (at 0 ms), while the helmet airbag is deployed when the acceleration on the X and Y axes reaches the threshold imposed by the manufacturer, in this case following the pelvis impact (at 172 ms, 123 ms before the head impact).

It has been determined that the late deployment of the helmet airbag was influenced by the longitudinal rear impact configuration, which generates a vertical motion for the cyclist between the vehicle-bicycle impact and the pelvis impact, undetectable by the airbag's deployment system since it is a vertical motion on the Z axis.

5. CONCLUSION

As presented, significant differences were determined in the current comparative analysis between the behavior of the tested airbags, in terms of both injury reduction and inflation performance.

The helmet airbag used in our study offered higher protection, in terms of both head and neck injury reduction with 46% and 32% respectively, but the deployment time was significantly higher than for the external airbag.

A downside of helmet airbags is indicated in the case of rear collisions with higher vehicle impact velocities. If the head impact time is inferior to the airbag debut time, then the inflation of the airbag is practically useless since head injuries are already produced.

Therefore, it is questionable if helmet airbags can provide safety to cyclists in these situations. Additional studies and airbag inflation optimizations are required in order to make helmet airbags feasible for protecting cyclists at higher impact velocities. Although the external airbag used in our study, designed to cover the upper extremity of the windscreen, determined higher injury criteria values than the helmet airbag, the debut inflation time of 93 ms indicates a significant potential for external airbags in offering protection at higher impact velocities. Additional research is required in order to increase injury mitigation potential, by optimizing the inclination and deployment time, as well as the volume and the pressure of the airbag.

REFERENCES

- [1] Alstin, Terese and Haupt, Anna, *System and method for protecting a bodypart*. Hovding Sverige AB. U.S. Patent 8,402,568, 2013
- [2] Bambach, R. Michael; Mitchell, R.J., Grzebieta, H. Rahael and Olivier, J., *The effectiveness of helmets in bicycle collisions with motor vehicles: A case-control study*. Accident Analysis and Prevention. vol. 53: pp. 78-pp.88, 2013.
- [3] Crompton, A. Peter; Dressler, M. Daniel; Stuart, A. Cameron; Dennison, R. Christopher and Richards, Darrin, *Bicycle helmets are highly effective at preventing head injury during head impact: Head-form accelerations and injury criteria for helmeted and unhelmeted impacts*. Accident; analysis and prevention, vol. 70, pp.1-pp.14, 2014.
- [4] Data Processing Vehicle Safety Group, *Crash Analysis Criteria Description Version 2*. Arbeitskreis Messdatenverarbeitung Fahrzeugischerheit. 2006
- [5] European Commission, *Flash Eurobarometer - Future of transport. Analytical report*. European Commission. Flash EB Series #312. 2010
- [6] European Commission, *Traffic Safety Basis Facts 2017 – Cyclists*. European Commission, 2017
- [7] Fredriksson Rikard and Rosén Erik, *Integrated pedestrian countermeasures - potential of head injury reduction combining passive and active countermeasures*. IRCOBI (International Research Council On the Biomechanics of Impact), pp.400-pp.407, 2010.
- [8] Hertz Ellen, *A note on the head injury criterion (HIC) as a predictor of the risk of skull fracture*. Proceedings: Association for the Advancement of automotive medicine annual conference, vol. 37, pp. 303-pp.312, 1993.
- [9] Kietlinski, Kajetan; Tijssens, Martin and Schüling, Jürgen, *Simulation of New Safety Measures to Protect Vulnerable Road Users*, AZT Worldw. vol. 119, 2017
- [10] Kurt, Mehmet; Laksari, Kaveh; Kuo, Calvin; Grant, A. Gerald and Camarillo, B. David, *Modeling and Optimization of Airbag Helmets for Preventing Head Injuries in Bicycling*. Annals of biomedical engineering, vol. 45(4), pp.1148-pp.1160, 2017.
- [11] Maki, Tetsuo; Kajzer, Janusz; Mizuno, Koji and Sekine, Yasufumi, *Comparative analysis of vehicle-bicyclist and vehicle-pedestrian accidents*. Accident Analysis & Prevention, vol. 35(6), pp.927-pp.940, 2003.
- [12] Matsui, Yasuhiro; Oikawa, Shoko and Hosokawa, Naruyuki, *Effectiveness of wearing a bicycle helmet for impacts against the front of a vehicle and the road surface*. Traffic Injury Prevention, vol. 19(7), pp.773-pp.777, 2018.
- [13] Olivier, Jake and Creighton, Prudence, *Bicycle injuries and helmet use: a systematic review and meta-analysis*. International Journal of Epidemiology vol.46(1): pp.278-pp.292, 2016.
- [14] Olsson, Dick and Sellergren, Ulf, *Airbag suitable for head protection*. Hovding Sverige AB. U.S. Patent Application 13/823,986, 2013
- [15] Otte Dietmar, *Possibilities and limitation for protective measures for injury reduction of vulnerable road users*. International Journal of Crashworthiness, vol. 7(4), pp.441-pp.462, 2002.
- [16] Rizzi, Mateo; Stigson, Helena and Krafft, Maria, *Cyclist injuries leading to permanent medical impairment in Sweden and the effect of bicycle helmets*. IRCOBI (International Research Council On the Biomechanics of Impact) Conference,, pp.412-pp.423, 2013.
- [17] Rodarius, Carmen; Mordaka, Justina and Versmissen, Ton, *Bicycle safety in bicycle to car accidents*. TNO. 2008
- [18] Stigson, Helena; Rizzi, Matteo; Ydenius, Anders; Engström, Emma and Kullgren Anders, *Consumer Testing of Bicycle Helmets*, IRCOBI (International Research Council On the Biomechanics of Impact) Conference,, pp.173-pp.181, 2017.

[19] Thompson, C. Diane; Rivara, Fred and Thompson, Robert, *Helmets for preventing head and facial injuries in bicyclists*. Cochrane Database of Systematic Reviews, 2000 (2), CD001855, 1999.

THE NEPCM MATERIAL AS COOLING SOLUTIONS FOR HIGH POWER LIGHT EMITTING DIODES (LED)

Dorin LELEA^{*}, Adrian Eugen CIOABLĂ

University Politehnica of Timisoara, B-dul Mihai Viteazu, Nr. 1, 300222 TIMISOARA, Romania

(Received 17 July 2018; Revised 21 August 2018; Accepted 15 September 2018)

Abstract. *The paper presents the thermal aspects of possibilities for using the Nano Encapsulated Phase Change Materials with the water as the base fluid as a cooling solution for high power light emitting diodes (LED). The approach used is based on the numerical modelling with control volume method as the theoretical background. The cooling device used in simulations is mini-channel heat sink with straight fluid flow channels. The results confirm the fact that Nano Encapsulated Phase Change Materials with the water as the base fluid, correlated with mini-channel heat sink, might be the suitable candidate for cooling of high power light emitting diodes (LED).*

Keywords: NEPCM, LED, cooling, numerical

1 INTRODUCTION

The cooling capabilities of Light Emitting Diodes (LED) might be improved with combine effect of microchannel heat sink and different nanofluids or PCM (phase change materials) slurries [1]. The issues associated with using Alumina nanofluid and n-Octadane NEPCM in double layer microchannel heat sink in laminar flow was analyzed by Rajabifar [2]. Sabbah et al [3] investigate numerically the heat transfer and fluid flow of Micro Encapsulated Phase Change Materials slurry in 3D microchannel heat sink. They have found that heat transfer coefficient increased significantly for heat flux of 100 and 500 W/cm². Kibria et al [4] and Jurkowska and Szczygiel presented review [5] on properties of NEPCM.

Hu and Zhang [6] presented the numerical research on laminar heat transfer and fluid flow in tubes of micro encapsulated phase change materials slurry. The results revealed that classical relations for Nu are not appropriate for estimation of heat transfer coefficient. Royon and Guiffant [7] presented the analytical approach on NEPCM slurry heat transfer and fluid flow through tubes with constant heat flux as boundary condition. It was found that Re has marginal influence on results.

Experimental research on heat transfer and fluid flow of NEPCM slurry through mini tubes was analyzed by Zhang and Ye [8] and Wu et al [9]. It is shown that homogeneous model is more appropriate for analyze. Moreover the heat transfer coefficient is two times greater than for base fluid.

Ma et al [10] investigate the heat transfer and fluid flow of clathrate hydrate slurry in straight tubes. It was found that heat transfer coefficient was enhanced 300 % compared to water. Kozak et al [11] investigated numerically and experimentally the heat transfer and fluid flow of hybrid air – PCM heat sink. It is revealed that this type of cooling is appropriate if latent heat prevails. Following the actual status of research in this area, thermal performance of the microchannel heat sink is analyzed numerically with NEPCM (n-Octadecane) – water slurry used as the cooling fluid. Two different melting ranges are considered: 10 K and 15 K. The analysis is made on a constant pumping power basis.

2 NUMERICAL DETAILS

The thermal management system of Light Emitting Diodes is presented in Figure 1, consisting of microchannel heat sink with NEPCM-water slurry as the cooling liquid.

The one-layer microchannel heat sink is presented in Figure 1.

For symmetry considerations, the half cross-section of one channel is analyzed.

^{*} Corresponding author e-mail: dorin.lelea@upt.ro

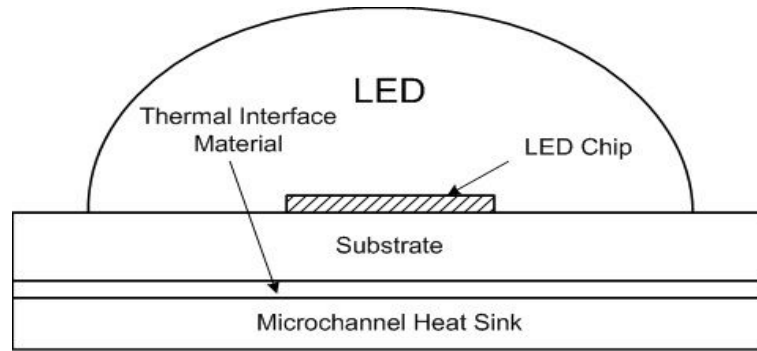


Figure 1. The LED cooling system

The set of the Navier-Stokes equations is used for the conjugate laminar steady state heat transfer and fluid flow, as follows:

The continuity equation:

$$\frac{\partial u}{\partial x} + \frac{\partial v}{\partial y} + \frac{\partial w}{\partial z} = 0 \quad (1)$$

The momentum equation:

$$\rho \left(u \frac{\partial u}{\partial x} + v \frac{\partial u}{\partial y} + w \frac{\partial u}{\partial z} \right) = -\frac{\partial p}{\partial x} + \left(\frac{\partial}{\partial x} \left(\mu \frac{\partial u}{\partial x} \right) + \frac{\partial}{\partial y} \left(\mu \frac{\partial u}{\partial y} \right) \right) \quad (2)$$

$$\rho \left(u \frac{\partial v}{\partial x} + v \frac{\partial v}{\partial y} + w \frac{\partial v}{\partial z} \right) = -\frac{\partial p}{\partial y} + \left(\frac{\partial}{\partial x} \left(\mu \frac{\partial v}{\partial x} \right) + \frac{\partial}{\partial y} \left(\mu \frac{\partial v}{\partial y} \right) \right) \quad (3)$$

$$\rho \left(u \frac{\partial w}{\partial x} + v \frac{\partial w}{\partial y} + w \frac{\partial w}{\partial z} \right) = -\frac{\partial p}{\partial z} + \left(\frac{\partial}{\partial x} \left(\mu \frac{\partial w}{\partial x} \right) + \frac{\partial}{\partial y} \left(\mu \frac{\partial w}{\partial y} \right) \right) \quad (4)$$

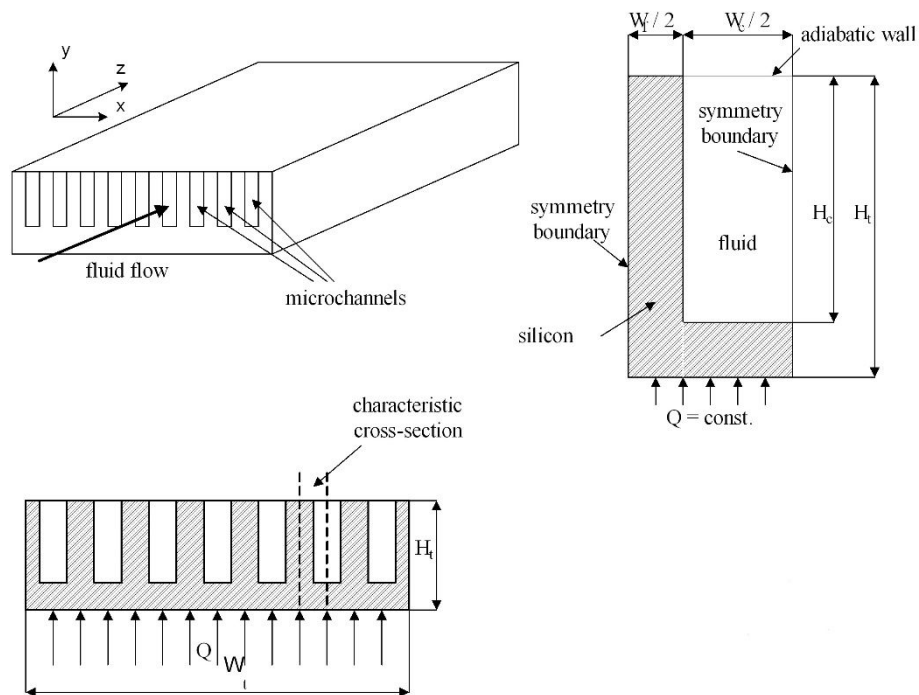


Figure 2. The microchannel heat sink used as cooling device

The energy equation (for both fluid and solid):

$$\rho \cdot c_p \cdot \left(u \frac{\partial T}{\partial x} + v \frac{\partial T}{\partial y} + w \frac{\partial T}{\partial z} \right) = k \left(\frac{\partial^2 T}{\partial x^2} + \frac{\partial^2 T}{\partial y^2} + \frac{\partial^2 T}{\partial z^2} \right) \quad (5)$$

The conjugate heat transfer procedure, implies the continuity of the temperature and heat flux at the solid – liquid interface defined as,

$$x = W_f/2: T_s|_{x+} = T_f|_{x-} \quad (6)$$

$$k_s \left(\frac{\partial T_s}{\partial x} \right)_{x+} = k_f \left(\frac{\partial T_f}{\partial x} \right)_{x-} \quad (7)$$

$$y = H_t - H_c: T_s|_{y+} = T_f|_{y-} \quad (8)$$

$$k_s \left(\frac{\partial T_s}{\partial y} \right)_{y+} = k_f \left(\frac{\partial T_f}{\partial y} \right)_{y-} \quad (9)$$

Also at the inlet cross-section, uniform velocity and temperature field are considered:

$$z = 0: u = u_{in} \quad \text{and} \quad T = T_{in} \quad (10)$$

The upper boundary is isolated defined as:

$$k \frac{\partial T}{\partial y} = 0 \quad (11)$$

At the outlet of the microchannel the following boundary conditions are prescribed:

$$z = L_t: \frac{\partial T}{\partial z} = 0 \quad (12)$$

At the symmetry boundary:

$$x = w_f/2 + w_d/2 \quad (13)$$

$$v = 0; \frac{\partial w}{\partial z} = 0; \frac{\partial u}{\partial z} = 0; \frac{\partial T}{\partial z} = 0 \quad (14)$$

The NEPCM – water static thermal conductivity [12]:

$$\frac{k_b}{k_{bf}} = \frac{2 + \frac{k_p}{k_f} + 2 \cdot \phi \cdot \left(\frac{k_p}{k_f} - 1 \right)}{2 + \frac{k_p}{k_f} - \phi \cdot \left(\frac{k_p}{k_f} - 1 \right)} \quad (15)$$

The effective thermal conductivity of the NEPCM – water slurry is defined as [13]:

$$\frac{k_{eff}}{k_b} = 1 + B \cdot \phi \cdot Pe_p^m \quad (16)$$

The particle Peclet number is defined as:

$$Pe_p = \frac{e \cdot d_p}{a_f} \quad (17)$$

The share rate is:

$$e = \frac{1}{2} \cdot \left(\frac{\partial u}{\partial r} - \frac{\partial v}{\partial z} \right) \quad (18)$$

The constants B and m are obtained from:

| | | |
|------------------------|------------|------------|
| For $Pep < 0.67$ | $B = 3,$ | $m = 1.5$ |
| For $0.67 < Pep < 250$ | $B = 1.8,$ | $m = 0.18$ |
| For $Pep > 250$ | $B = 3,$ | $m = 1/11$ |

The effective viscosity of NEPCM – water slurry is defined as [14]:

$$\frac{\mu_{eff}}{\mu_{bf}} = (1 - \phi - 1.16 \cdot \phi^2)^{-2.5} \quad (19)$$

The effective density is defined as:

$$\rho_{eff} = (1 - c_m) \cdot \rho_f + c_m \cdot \rho_{pcm} \quad (20)$$

The effective specific heat is calculated as:

$$c_{peff} = \frac{(1 - c_m) \cdot (\rho \cdot c_p)_f + c_m \cdot (\rho \cdot c_p)_{pcm}}{\rho_{eff}} \quad (21)$$

The specific heat of the NEPCM particle is calculated from the sine profile [15]:

$$c_{p,p} = c_{p,s} + \left\{ \frac{\pi}{2} \left(\frac{h_{sf}}{\Delta T_m} - c_{p,s} \right) \cdot \sin \pi \cdot \left[\frac{(T - T_l)}{\Delta T_m} \right] \right\} \quad (22)$$

Relation between the volume and mass concentration of the nanoparticles might be obtained from:

$$c_m = \frac{\phi \cdot \rho_p}{(\rho_f + \phi \cdot (\rho_p - \rho_f))} \quad (23)$$

Re is defined as:

$$Re = \frac{\rho_{eff} \cdot u_m \cdot D_i}{\mu_{eff}} \quad (24)$$

The pumping power is defined as [16]:

$$\Pi = M \cdot \frac{\Delta p}{\rho_{eff}} \quad (25)$$

The solution procedure is based on the method used in [17] for microtubes and on the Finite Volume Method described in [18]. Also k acts as k_s for silicon wall and k_f in the case of the water. At the fluid – solid interface k is calculated as the harmonic mean value. The velocity-pressure coupling is solved using a *SIMPLER* method. A staggered grid is used for cross-stream velocities with power-law discretization scheme.

3 RESULTS AND DISCUSSION

The scope of research was to make the appropriate performance evaluation of the microscale device using NEPCM-water slurry with different melting ranges and same particle diameter. Generally speaking there are two different base criteria that might be employed, the fixed pumping power and fixed Re. Besides the numerical results are presented in terms of maximum temperature of the substrate that might be used for evaluation of the thermal resistance. The numerical results are presented in Figure 3. Two different values for melting range are presented, $\Delta T_m = 10$ and 15 K. Moreover the results are compared with those obtained for Al₂O₃-water nanofluid for volume concentration of $\rho = 2\%$ and particle diameter of $d_p = 20$ nm. For the same pumping power $\Pi = 1$ W, the local temperature distribution along the substrate is lower in case of NEPCM-water slurry compared with water based Al₂O₃ nanofluid. Maximum temperature difference is up to 10 K. Moreover temperature difference between two ΔT_m is negligible.

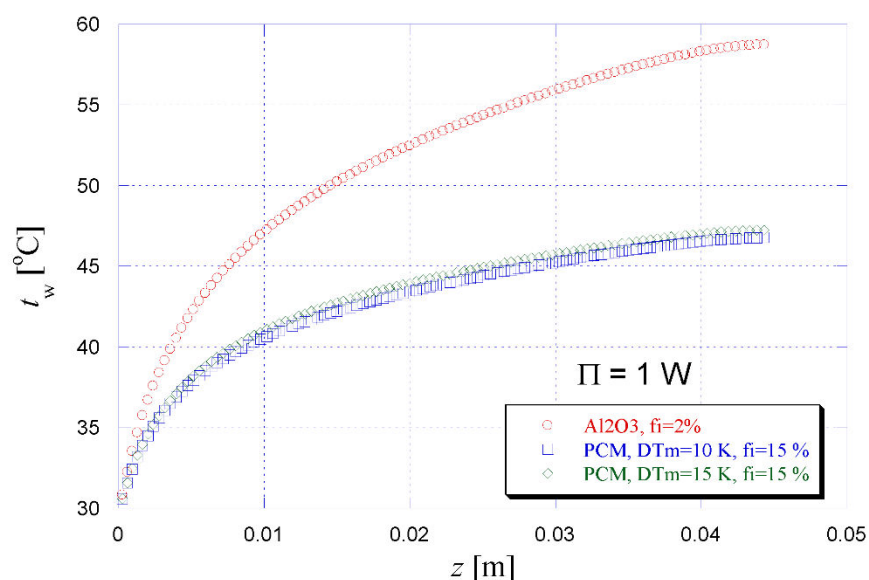


Figure 3. The local wall temperature distribution

4 CONCLUSIONS

The research presented in the paper dealt with the heat transfer and fluid flow of microchannel heat sink using the NEPCM (n-Octadecane) – water slurry cooling medium. Considering that the melting range of phase change material has important impact on heat sink thermal performance, two different values are considered: 10 K and 15K. The results are compared with Al₂O₃ water based nanofluid in terms of constant pumping power basis. Two main conclusions can be emphasized through presented results:

- The substrate temperature is lower for NEPCM-water slurry for both melting range differences considered in this paper;
- Difference in term of local temperature distribution between the melting ranges is negligible.

REFERENCES

- [1] Alquaity A.B.S., Al-Dini S.A., Yilbas B.S.: *Investigation into thermal performance of nanosized phase change material (PCM) in microchannel flow*. Int J Numer Method 23(2) 233-247 (2013)
- [2] Rajabifar B.: *Enhancement of the performance of a double layered microchannel heatsink using PCM slurry and nanofluid coolants*. Int J Heat Mass Tran 88, 627-635 (2015)
- [3] Sabbah R., Farid M. M., Al-Hallaj S.: *Micro-channel heat sink with slurry of water with micro-encapsulated phase change material: 3D-numerical study*. Applied Thermal Engineering 29, 445–454 (2008)
- [4] Kibria M.A., Anisur M.R., Mahfuz M.H., Saidur R., Metselaar I.H.S.C.: *A review on thermophysical properties of nanoparticle dispersed phase change materials*. Energy Conversion and Management 95, 69–89 (2015)
- [5] Jurkowska M., Szczygiel I.: *Review on properties of microencapsulated phase change materials slurries (mPCMS)*. Applied Thermal Engineering 98, 365–373 (2016)
- [6] Hu X., Zhang Y.: *Novel insight and numerical analysis of convective heat transfer enhancement with microencapsulated phase change material slurries: laminar flow in a circular tube with constant heat flux*. International Journal of Heat and Mass Transfer 45, 3163–3172 (2002)
- [7] Royon L., Guiffant G.: *Forced convection heat transfer with slurry of phase change material in circular ducts: A phenomenological approach*. Energy Conversion and Management 49 928–932 (2008)
- [8] Zhang P., Ye J.: *Experimental investigation of forced flow and heat transfer characteristics of phase change material slurries in mini-tubes*. International Journal of Heat and Mass Transfer 79, 1002–1013 (2014)
- [9] Wu W., Bostanci H., Chow L.C., Hong Y., Wang C.M., Su M., Kizito J.P.: *Heat transfer enhancement of PAO in microchannel heat exchanger using nano-encapsulated phase change indium particles*. International Journal of Heat and Mass Transfer 58, 348–355 (2013)
- [10] Ma Z.W., Zhang P., Wang R.Z., Furui S., Xi G.N.: *Forced flow and convective melting heat transfer of clathrate hydrate slurry in tubes*. International Journal of Heat and Mass Transfer 53, 3745–3757 (2010)
- [11] Kozak Y., Abramzon B., Ziskind G.: *Experimental and numerical investigation of a hybrid PCMeair heat sink*. Applied Thermal Engineering 59, 142 -152 (2013)
- [12] Charunyakorn P., Sengupta S., Roy S.K.: *Forced convection heat transfer in microencapsulated phase change material slurries: flow in circular ducts*. Int J Heat Mass Tran 34(3), 819 - 833 (1991)
- [13] Vand V.: *Theory of viscosity of concentrated suspensions*, Nature, 155 (1945) 364-365
- [14] Alisetti E.L., Roy S.K.: *Forced convection heat transfer to phase change material slurries in circular ducts*. J. Thermophys. Heat Transfer 14(1), 115–118 (2000)
- [15] Bayramoglu E.Ç.I.: *Thermal properties and stability of n-octadecane based composites containing multiwalled carbon nanotubes*. Polymer Composites 32(6), 904-909 (2011)
- [16] Milanović P., Jaćimović B., Genić S.: *The influence of heat exchanger performances on the design of indirect geothermal heating system*. Energy And Buildings 36(1), 9-14 (2004)
- [17] Lelea D.: *The heat transfer and fluid flow of a partially heated microchannel heat sink*. International Communications in Heat and Mass Transfer 36, 794–798 (2009)
- [18] Patankar S.V.: *Numerical Heat Transfer and Fluid Flow*. McGraw Hill, New York (1980)

EFFICIENCY ANALYSIS OF PASSIVE SAFETY SYSTEMS IN VEHICLES IN THE CASE OF FRONTAL COLLISION USING EXPERIMENTAL TESTS

Alexandru Ionut RADU^{1)*}, Daniel Dragos TRUSCA¹⁾, George TOGANEL¹⁾, Bogdan TOLEA²⁾

¹⁾ Transylvania University of Braşov, Str. Politehnicii Nr. 1, 500024 BRASOV, Romania

²⁾ University of Oradea, ORADEA, 410610, Romania

(Received 10 July 2018; Revised 21 August 2018; Accepted 14 September 2018)

Abstract: The main objective was to study the efficiency of airbag and seatbelt combination in a frontal collision between two passenger vehicles by the means of experimental crash tests. To do this, we conducted crash tests in a controlled environment and in the vehicles there were crash test dummies to simulate the human occupant. Two experimental crash tests were conducted at the velocity of 35 km/h, where 1 set of vehicles used passive safety systems and 1 set did not have these systems. The occupants of the vehicles were custom build crash test dummies that resemble an average male human and have close characteristics to the Hybrid III 50th percent male dummy. The dummy head acceleration was measured and the injury potential was calculated using the head injury criteria in both cases (with and without an airbag). We predict that by using passive safety systems, the injury potential to the occupants will be reduced and by measuring the head acceleration, we could calculate the head injury criteria (HIC) and estimate the probability of injury based on the HIC values.

Key-Words: Passive safety, Crash-test, Airbag, Seatbelt, Dummy

NOMENCLATURE

HIC: Head Injury Criteria

t_1 : initial time, s

t_2 : final time, s

a : acceleration, m/s^2

a_{rez} : resultant acceleration, m/s^2

a_x : acceleration value on the X axis, m/s^2

a_y : acceleration value on the Y axis, m/s^2

a_z : acceleration value on the Z axis, m/s^2

t : time, s

1. INTRODUCTION

Frontal collisions are considered deadly due to the fact that both vehicles are traveling in opposite directions cumulating the impact velocity [1]. This happens very often on highways or on 2 lane roads when a vehicle is engaged in a passing maneuver, not estimating the correct distance and unable to retreat in time, colliding with the opposing vehicle [2]. Since its introduction on passenger vehicles, seat belts have been very effective systems to protect the occupants in case of a collision. In Europe the standard setup of the seat belt is the three point configuration, covering the lap and shoulder of the passengers [3][4][5]. It has been proven that the seatbelt will save the passenger's life if it is used, and not using it in the same circumstances will lead to death [6][7]. Along with the seatbelts, airbags have shown to have a good protection of the occupant head [8]. Huere has studied in a study that airbags can reduce head injuries by up to 82% for the 56-65 km/h range [9]. Using the airbag, it was demonstrated that in 85% of cases, head injuries were classified as minor injuries [10]. In order to obtain a probability of injury for the study, the head injury criterion was used.

* Corresponding author e-mail: alexandru.radu@unitbv.ro

The head injury criterion can be presented by a parameter called HIC, defined by a mathematical formula. The HIC criterion is a way of assessing the risk of a cranial trauma injury as a result of an accident. It can be used to assess the consequences of traffic accidents, testing individual protection equipment or safety sports equipment [11].

The HIC criterion is the maximum standard value of the integral of the head acceleration. Depending on the interval for which it is calculated, the HIC criterion is:

- Unlimited - HIC;
- 36 ms maximum - HIC36;
- Maximum 15 ms - HIC15.

The mathematical formula for determining the HIC criterion is [12][13].

$$HIC = \left\{ \left[\frac{1}{t_2 - t_1} \int_{t_1}^{t_2} a \cdot dt \right]^{2.5} \cdot (t_2 - t_1) \right\}_{MAX} \quad (1)$$

Where a is the resulting acceleration of the center of gravity of the head, measured in m/s^2 , and t_1 and t_2 are the time interval (s) in which HIC has the maximum value. An important observation is that HIC is dimensionless.

The Abbreviated Injury Scale (AIS) is a system for assessing the degree of injury of occupants involved in traffic accidents by expressing injuries in the form of categories numbered 1 to 6 depending on their severity, from minor injuries marked with 1 to serious lesions that can cause death, marked with 6 [14]. Based on a set of experiments a correlation was made between the value of the HIC and the AIS scale. Note that this correlation is based only on impact tests where head injuries have been analyzed. The correlation is presented in a graphical form [15].

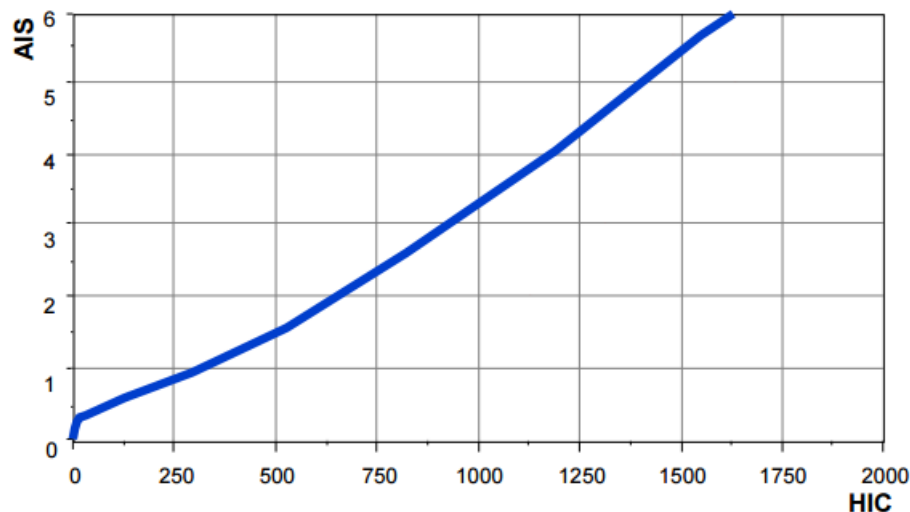


Figure 1. Correlation between HIC and AIS scale

In this study the kinematics of the occupant were analysed and the head-neck angles were measured during the collision. There are tolerances for the neck's flexion and extensions phases. Arun determined the normal cervical motion interval for the following phases [16][17]:

- Flexion - 80 to 90 degrees;
- Extension - 70 degrees;
- Side flexion - 20 to 45 degrees on both sides;
- Rotation - 90 degrees of rotation in both directions.

In order to calculate the HIC values, the resulting head acceleration values were needed. To obtain these values, the following formula was used [18][19]:

$$a_{rez} = \sqrt{a_x^2 + a_y^2 + a_z^2} \quad (2)$$

Where:

a_{rez} – resultant acceleration;
 a_x – acceleration values on the X axis;
 a_y – acceleration values on the Y axis;
 a_z – acceleration values on the Z axis.

2. METHODOLOGY

The methodology used for the study of this paper consisted of conducting experimental tests involving frontal vehicle collisions with crash test dummies.

A few objectives were set that resulted from the experimental tests.

The following objectives were set:

- Determination of collision dynamics - impact phase analysis;
- Analysis of kinematic parameters during collision;
- Determining the degree of injury to the occupants using the HIC injury criterion and correlating the values with the AIS severity scale.

For this study, four vehicles were used, 2 were stationary with the crash test dummies inside and 2 were used as striking vehicles.

The test scenarios are presented in figure 2. The collisions were filmed using high speed video cameras. Two cameras were used, a Casio Exilium, capable of capturing up to 500 FPS and a Fastech Hispec 5, capable of filming up to 1000 FPS.

The video was used to analyze the kinematics and dynamics of the vehicles and occupant during the collision.

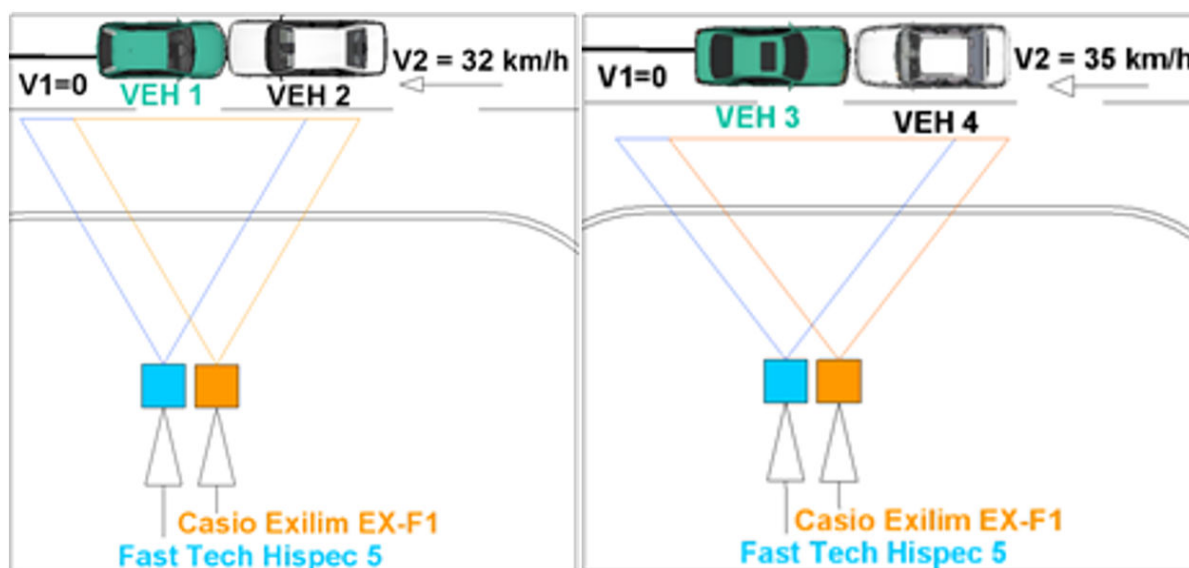


Figure 2. Test scenarios used: Frontal collision without airbag (left) and frontal collision with airbag and pretensioned seatbelt (right)

For the first test, the vehicle where the occupant was had no airbag, only the seatbelt, without pretensioning system. On the second test, the vehicle with the occupant was equipped with front airbag mounted in the steering wheel along with a pretensioning system for the seatbelt in order to secure the occupant during the collision.

The kinematics of the vehicles during the collision is presented in figure 3.

In the figure above there are 3 phases presented for both collisions.

Phase 1 represents the pre-impact position of the vehicles, phase 2 is the collision phase where the energy is transferred and the occupant moves inside the vehicle and phase 3 is the post-impact phase in which the vehicles detach.

On the second test (right) we can see the airbag completely deployed during the collision phase.



Figure 3. Accident kinematic of the two tests

3. RESULTS

The primary results of the study are presented in the next figures. The key parameter was the head acceleration values of the occupants. These values will help determine the injury potential of head. For the first test, where there wasn't an airbag, the head acceleration is presented in figure 4.

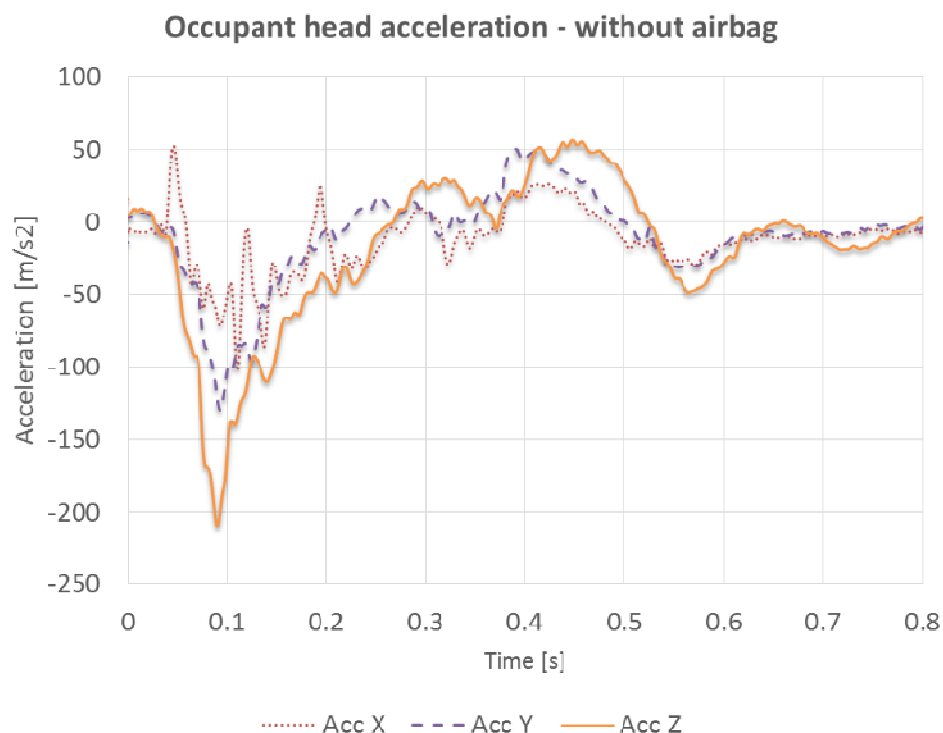


Figure 4. Acceleration values for the occupant's head in the first test (without airbag)

In the figure it can be observed that the peak maximum value of the acceleration was 220 m/s² on the Z axis during the first 100 ms of the collision. On the Y axis, the maximum acceleration was 130 m/s². In the next figure, the head acceleration values are presented for the second test where the vehicle had an airbag and seatbelt pretensioner.

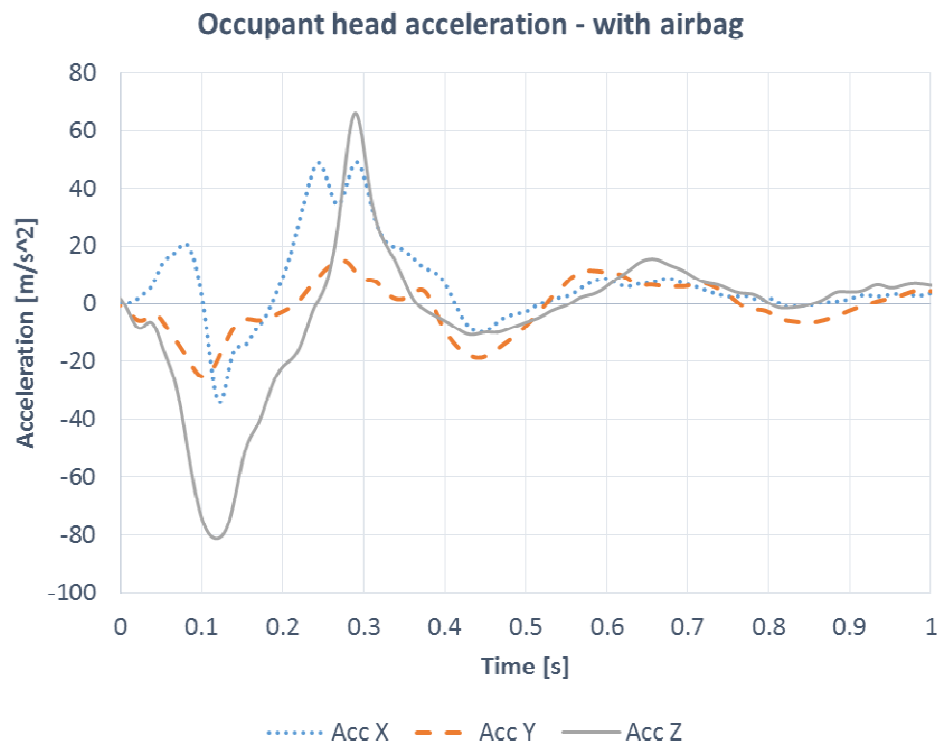


Figure 5. Acceleration values for the occupant's head in the second test (with airbag)

In this test, it is observed that the maximum acceleration value was much lower compared to the first test. The maximum value was 80 m/s² on the Z axis, during the first 150 ms. In this test, another peak value is seen of 62 m/s², between 200 – 350 ms, caused by the occupant head hitting the headrest after the recoil from the airbag. In order to calculate the HIC 36 values for the two test, the acceleration resultant is required. So for the first test, the acceleration resultant is presented in figure 6.

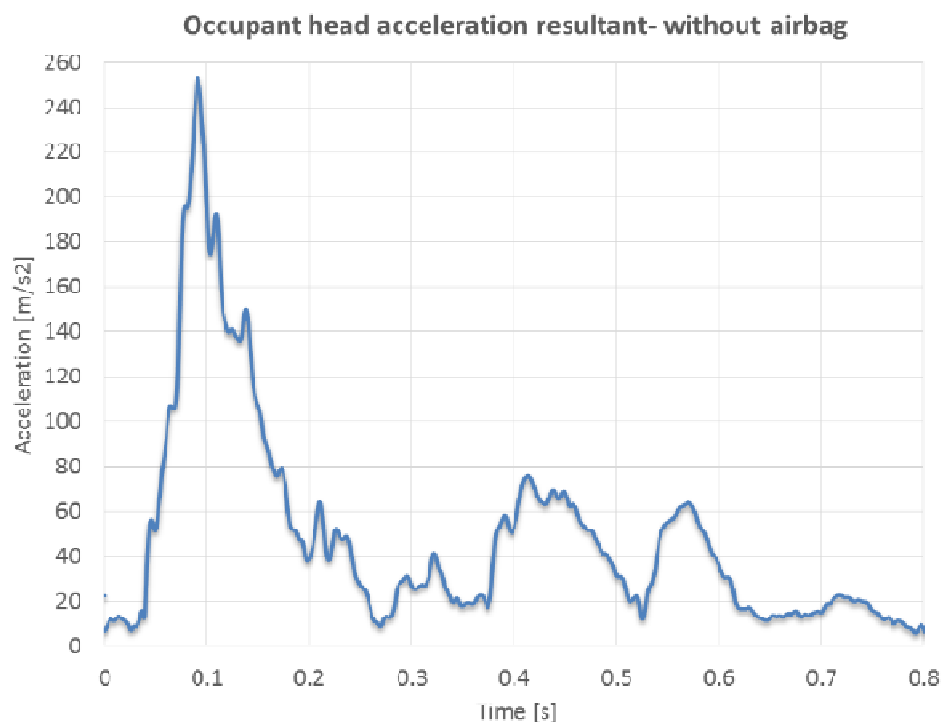


Figure 6. Acceleration resultant for the first test

By obtaining the resultant, the maximum acceleration value is 251 m/s² for the first test during the first 100 ms of the collision. For the second test, the acceleration re-sultant is also calculated.

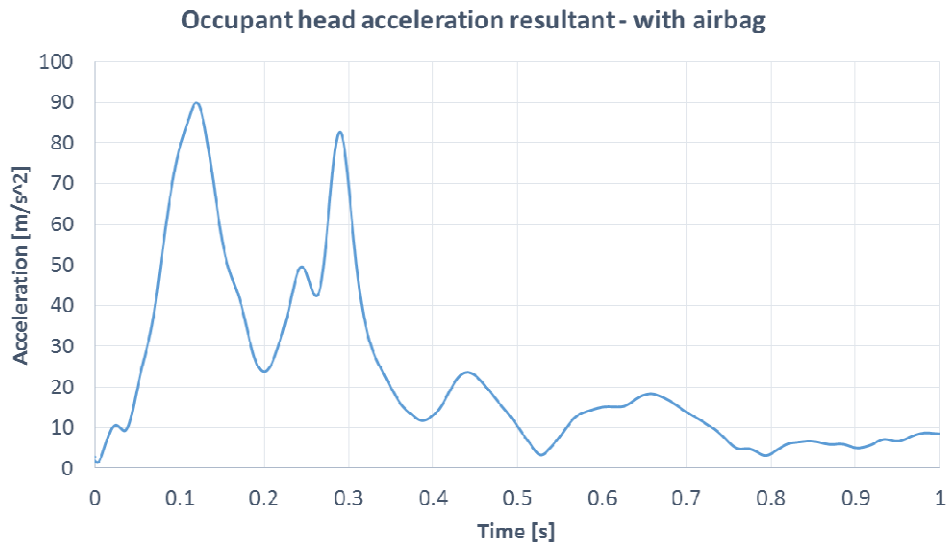


Figure 7. Acceleration resultant for the second test

In this case, we can see the 2 peaks mentioned earlier, the first peak, with the value of 90 m/s², during the first 150 ms, is caused by the initial collision and impact of the head with the airbag. The second peak, with the value of 82 m/s², between 250 – 300 ms, is caused by the impact of the head with the headrest. After calculating the head acceleration of the occupant for both tests, the HIC values were calculated using the HIC formula with the time lapse of 36 ms.

For the first test, the HIC calculation is presented in figure 8.

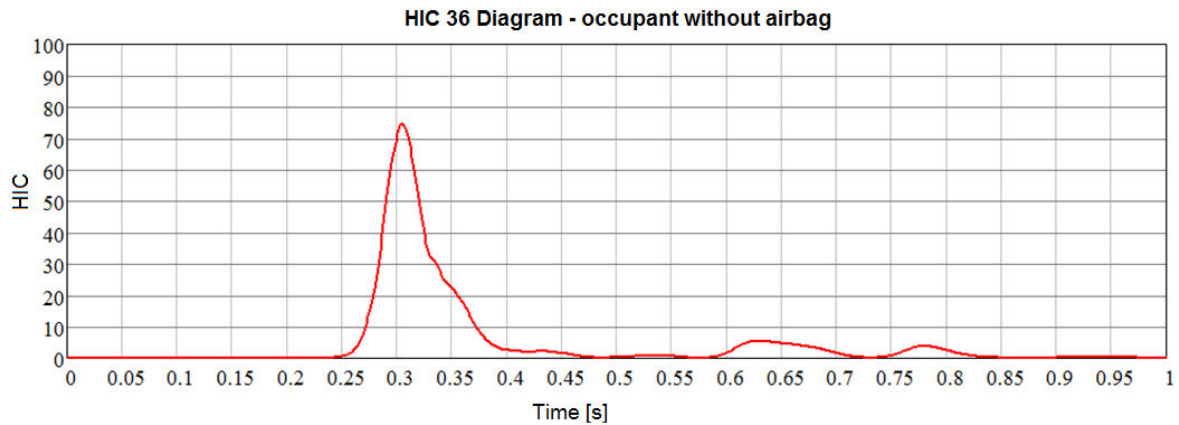


Figure 8. HIC 36 calculation for the first test (without airbag)

Using the HIC formula, the maximum value is presented below.

$$HIC36_1 = \max_{t_1 t_2} \left(\left[\frac{1}{t_2 - t_1} \cdot \int_{t_1}^{t_2} a_{rez}(t) dt \right]^{2.5} \cdot (t_2 - t_1) \right) = 75 \quad (3)$$

The maximum value was 75, which in this case is low, compared to the maximum tolerance of the human body of HIC = 1000 and classifies the injury as AIS-1 (minor injuries) on the AIS scale.

For the second test, the HIC value diagram is presented below.

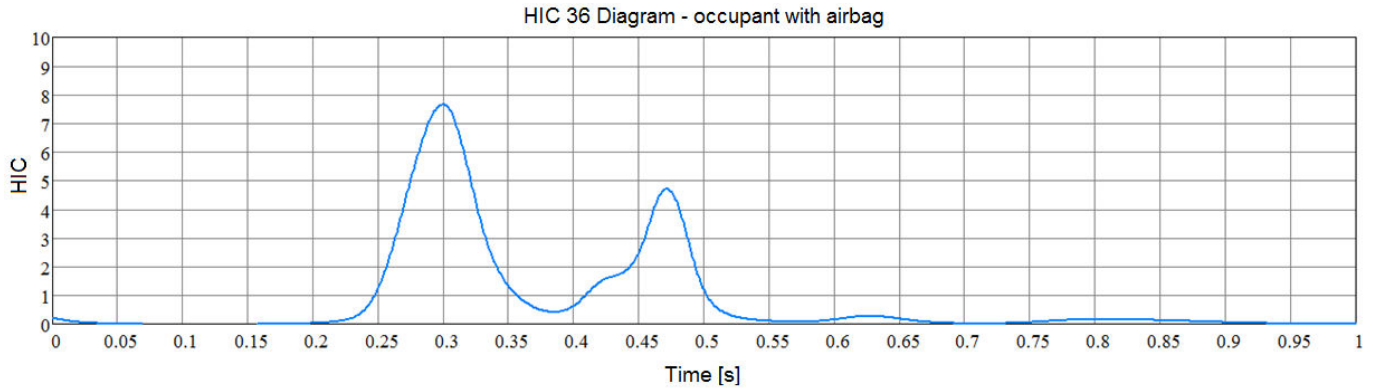


Figure 9. HIC 36 calculation for the second test (with airbag)

Using the HIC formula, the maximum value is presented below.

$$HIC36_2 = \max_{t_1 t_2} \left(\left[\frac{1}{t_2 - t_1} \cdot \int_{t_1}^{t_2} a_{rez}(t) dt \right]^{2.5} \cdot (t_2 - t_1) \right) = 7.7 \quad (4)$$

In this case the value is also very low, of 7.7 and classifies the head injury potential as AIS-1 (minor injury) on the AIS scale. By summing up the results and correlating the HIC values with the AIS scale, the probability potential was obtained and presented in figure 10.

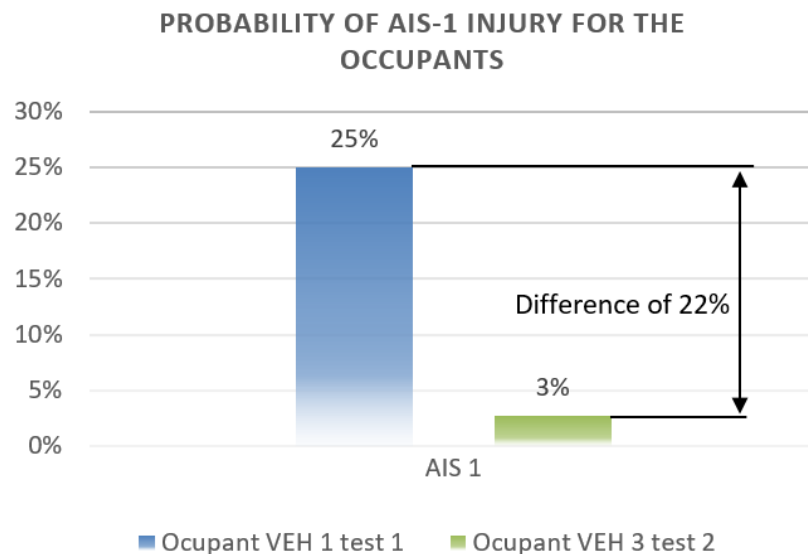


Figure 10. Injury probability for the occupants

In the first test, where there was no airbag, just the seatbelt, the occupant had a 25% probability of injury while in the second test where the airbag was activated, the injury potential was very low, of only 3%. The difference between the 2 tests is 22%, thus granting a reduction of 150% in injury probability. Also for this study, by using the high speed video recording, the occupant's movement was analyzed during impact. The angular displacement of the head relative to the chest was measured as well as the position of the thorax relative to the pelvis. The kinematics analysis phases were divided into 4 time periods. The times T0 and T3 respectively, represent the time of the first contact between the vehicles and the time of their detachment. Moments T1 and T2 represent the intermediate times in which milestones are essential (start the occupant's movement, reaching the maximum angular displacement for the head or torso).

In figure 11 the kinematic analysis for the first test is presented.

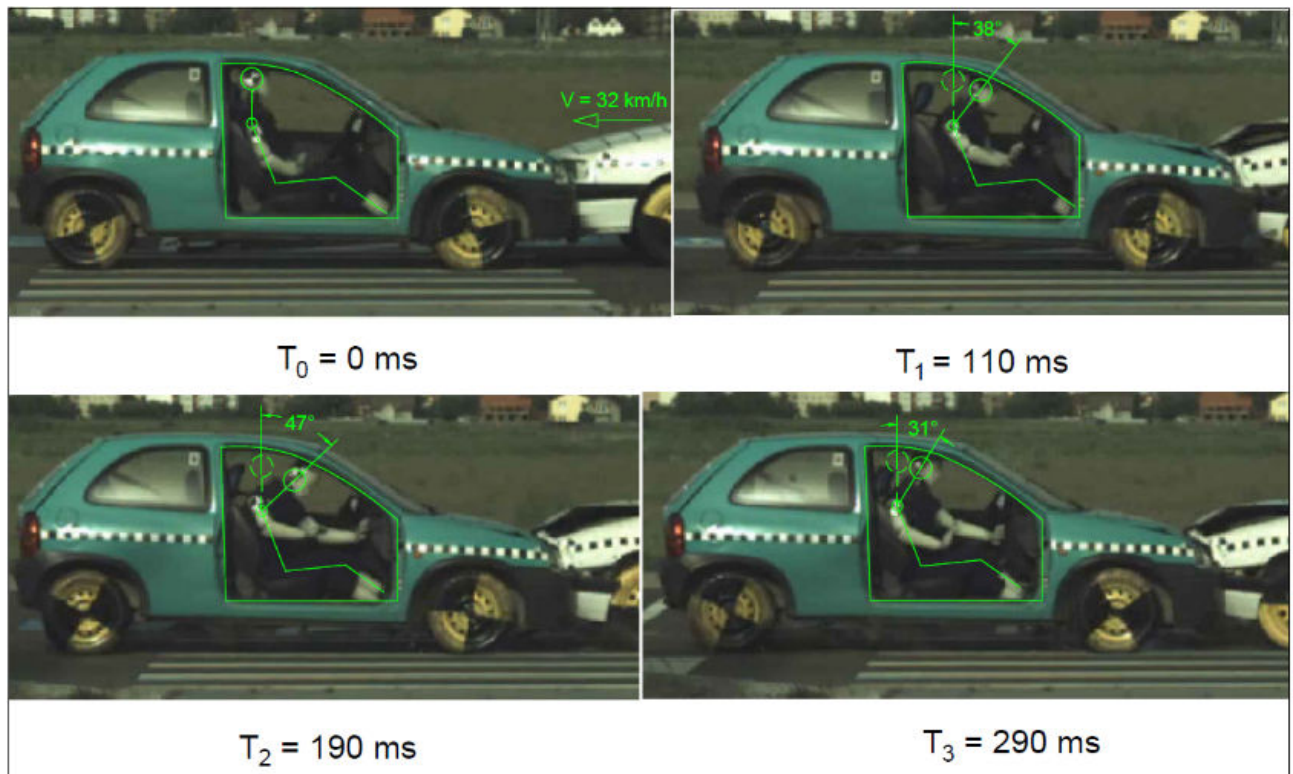


Figure 11. Kinematic analysis of the occupant during the first test

In the figure, at T1, the head of the occupant flexes forward due to the collision at an angle of 38 degrees relative to the torso and at T2 the maximum value of the head flexion is reached, with the value of 47 degrees. When the vehicles detach at T3, the head returns to its initial position.

These angles are considered normal and do not cause further injuries to the occupant. In the figure below, the kinematics for the second test are presented.

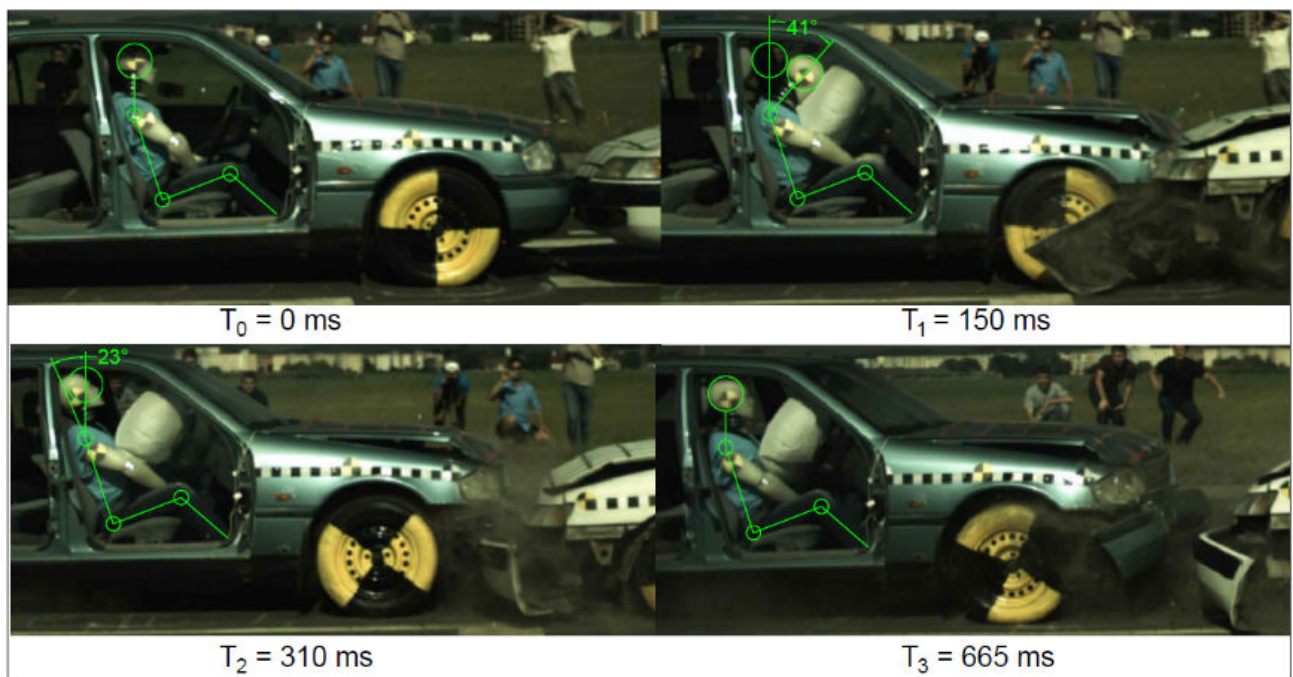


Figure 12. Kinematic analysis of the occupant during the second test

In this case, at T1, the head – torso angle was 41 degrees, during the flexion of the neck, limited by the deployment of the airbag that causes a recoil of the head, generating an extension phase for the neck and an angle of 23 degrees as seen at T2. When the vehicles detach, the head returns to its original position.

4. CONCLUSION

From the results shown it can be concluded that in low speed impacts such as the ones presented, the passive safety systems can make a difference in reducing the injury potential of the head.

Even though the injury potential calculated was minor, the tests demonstrate that the passive safety systems in today's vehicles will reduce the severity level for the driver of the vehicle.

The occupant movement in both tests showed similar angular values of the head (47 degrees and 42 degrees respectively) during the neck flexion stage. This was caused by the seatbelt keeping the occupant in the seats and the head and neck flexed forward.

Following the processing of the results from the frontal collision test (test 2) in which passive safety systems were used, it was found that the displacement of the head was limited by contact with the airbag.

Head Injury Criteria (HIC) values for frontal collision tests (Test 1 and 2) showed that the risk of injury to the occupant was minor (AIS-1 code) with a 25% probability of injury in case of absence of airbag.

With passive systems present (airbag and pretensioning belt), the risk of lesion decreases to 3%.

REFERENCES

- [1] Jarašūniene, A., Jakubauskas, G. *Improvement of road safety using passive and active intelligent vehicle safety systems*, Transport, 22(4), 284-289, 2007.
- [2] Elmarakbi, A. M., Zu, J. W. *Crash analysis and modeling of two vehicles in frontal collisions using two types of smart front-end structures: an analytical approach using IHBM*, International Journal of Crashworthiness, 11(5), 467-483, 2006.
- [3] Van Houten, R., Malenfant, J. E., Austin, J., Lebbon, A. *The Effects of a Seatbelt-Gearshift Delay Prompt on the Seatbelt Use of Motorists Who Do Not Regularly Wear Seatbelts*, Journal of applied behavior analysis, 38(2), 195, 2005.
- [4] Abbas, A. K., Hefny, A. F., Abu-Zidan, F. M. *Seatbelts and road traffic collision injuries*, World journal of emergency surgery, 6(1), 18, 2011.
- [5] Yano, H., Tanaka, K., Tanji, H. U.S. Patent No. 6,726,249. Washington, DC: U.S. Patent and Trademark Office, 2004.
- [6] Geller, E. S., Paterson, L., Talbott, E. *A behavioral analysis of incentive prompts for motivating seat belt use*, Journal of Applied Behavior Analysis, 15(3), 403-413, 1982.
- [7] Slovic, P., Fischhoff, B., Lichtenstein, S. *Accident probabilities and seat belt usage: A psychological perspective*, Accident Analysis & Prevention, 10(4), 281-285, 1978.
- [8] Gabauer, D. J., Gabler, H. C. *The effects of airbags and seatbelts on occupant injury in longitudinal barrier crashes*, Journal of safety research, 41(1), 9-15, 2010.
- [9] Huère, J. F., Foret-Bruno, J. Y., Faverjon, G. *Airbag efficiency in frontal real world accidents*, In Proceedings: International Technical Conference on the Enhanced Safety of Vehicles (Vol. 2001, pp. 6-p). National Highway Traffic Safety Administration, 2001.
- [10] Huère, Jean-François, et al. *Airbag efficiency in frontal real world accidents*, No. 2001-06-0010. SAE Technical Paper, 2001.
- [11] Gao, Dalong, Charles W. Wampler. "Head injury criterion." IEEE robotics & automation magazine 16.4: 71-74, 2009.
- [12] McHenry, B. G. *Head injury criterion and the ATB*, ATB Users' Group, 5-8, 2004.
- [13] Eppinger, Rolf, et al. *Supplement: Development of improved injury criteria for the assessment of advanced automotive restraint systems-II*, National Highway Traffic Safety Administration, 2000.
- [14] Greenspan, L., McLELLAN, B. A., Greig, H. *Abbreviated Injury Scale and Injury Severity Score: a scoring chart*, The Journal of trauma, 25(1), 60-64, 1985.
- [15] Prasad, P., Mertz, H. J. *The position of the United States delegation to the ISO Working Group 6 on the use of HIC in the automotive environment*, (No. 851246). SAE Technical Paper, 1985.

- [16] Arun, P. S. *Range of Motion of Cervical Spine*, <http://boneandspine.com/range-motion-cervical-spine/> 2016/10/18.
- [17] Joumana, M. *Human Anatomy Fundamentals: Flexibility and Joint Limitations*, <http://design.tutsplus.com/articles/human-anatomy-fundamentals-flexibility-and-joint-limitations--vector-25401,2014>.
- [18] Ewing, C. L., Thomas, D. J., Lustick, L., Becker, E., Williams, G. *The effect of the initial position of the head and neck on the dynamic response of the human head and neck to-Gx impact acceleration*, NAVAL AEROSPACE MEDICAL RESEARCH LAB DETACHMENT MICHOU D NEW ORLEANS LA, 1975.

DESIGN OPTIMIZATION OF A PASSENGER CAR'S STEERING SYSTEM FOR MINIMIZING THE ACKERMAN ERROR AND THE TURNING RADIUS

Augustin CONSTANTINESCU*, Mario TROTEA, Loreta SIMNICEANU, Gheorghe POPA-MITROI

University of Craiova, Calea București, Nr. 107, 200512 CRAIOVA, România

(Received 10 June 2018; Revised 21 July 2018; Accepted 14 August 2018)

Abstract. *The paper presents the design optimization of a passenger car's steering system for minimizing the Ackermann error and the turning radius during steering maneuvers. The virtual models of the suspension system and the steering system have been made using ADAMS/Car software. Both systems were configured based on a compact class passenger car. The positions of the spherical joint on the three axles of the lower control arm and the positions of the outer joint on the three axles of the steering tie rod were chosen as design variables. The objectives of the design optimization analysis were the Ackermann error and the turning radius, both to be minimized. By minimizing the Ackermann error, the front wheels will have less side slippage during cornering so the wear of the tire will be reduced. For urban passenger cars the turning radius of the car is an important factor for the car's maneuverability so minimizing it is a positive aspect. For both the virtual models (initial and optimized) the Ackermann error and the turning radius variation were plotted.*

Keywords: Ackermann Error, Steering Analysis, Turn Radius

1. INTRODUCTION

The steering system of the vehicles is based on the Ackerman geometry, which involves pure rolling with no lateral slippage of the front wheels in cornering. The Ackerman condition for two-axle vehicles requires that the axes of the front wheels intersect with the axis of the rear wheels on the same point. Failure to comply with this condition, even at low speed, produces, in addition to wheels rolling, a lateral slippage of the front wheels.

Zhou, Li and Yang [1] presented a design optimization of the steering system to reduce the Ackerman error and the variation of the toe angle with parallel travel of the front wheels, using the coordinates of the spherical joints of the tie rod as design variables.

Sleesongsom and Bureerat [2] presented a multi-objective optimization of the steering system to reduce the Ackerman error and the turning radius using an evolutionary algorithm for numerical solving of the optimal problem. Various studies for the steering system were also carried out in [3][4][5][6][7][8][9].

This paper presents the design optimization of the steering linkage to reduce the Ackerman error, respectively, the lateral slippage of the front wheels leading to additional tire wear, and the turning radius using ADAMS Car commercial software.

2. ACKERMAN STEERING GEOMETRY

When cornering, without lateral slippage, the center of the rigid wheel is always in its median plane. Whether the wheel centers are stationary in relation to the body, which can be considered rigid, means that the perpendiculars on median planes in these centers are intersecting in the center of the rotation [10]. Also, in the case of front wheels with spindle, where the wheel centers are not stationary in relation to the bodywork, the above property retains its validity [10]. For the case of a rigid wheels vehicle, their position when turning can be seen from the turning diagram shown in Figure 1.

The instantaneous rotation center, marked with C_v , is located on the rear axle axis and represents the center of the car's turn.

* Corresponding author e-mail: gusti_constantinescu@yahoo.com

The steering angle of the steered wheels, denoted by θ_e for the outer wheel and θ_i for the inner wheel of the turn, are different.

According to the scheme presented in Figure 1, for the two angles, the relations can be written:

$$\operatorname{tg} \theta_e = \frac{L}{R_v + 0,5E_p}, \quad \operatorname{tg} \theta_i = \frac{L}{R_v - 0,5E_p} \quad (1)$$

where

- R_v represents the turning radius, E_p is the distance between the left and right outer spherical joints of the lower control arm, measured in the transversal median plane of the wheels, and L is the vehicle's wheelbase.

Writing the difference between the two reversed equations it follows:

$$\operatorname{ctg} \theta_e - \operatorname{ctg} \theta_i = \frac{E_p}{L} \quad (2)$$

Equation (2) is known as Ackermann's condition, required for the correct ride of the front rigid wheels. Ackerman error is the difference between the steer angle and the ideal steer angle for Ackerman geometry. Because Adams Car uses the inside wheel to compute the turn center, the Ackerman error for the inside wheel is zero. For a left turn, the left wheel is the inside wheel and the right wheel is the outside wheel. Conversely, for a right turn, the right wheel is the inside wheel and the left wheel is the outside wheel. Positive Ackerman error indicates the actual steer angle is greater than the ideal steer angle or the actual is steered more to the right [11]. For calculating the minimum radius kerb-to-kerb according to the mean turning radius, the scheme of the cornering car is shown in Figure 2.

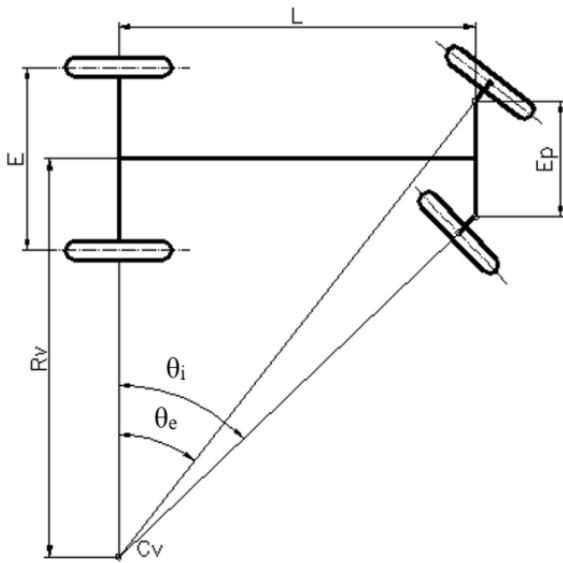


Figure 1. Ackerman steering geometry

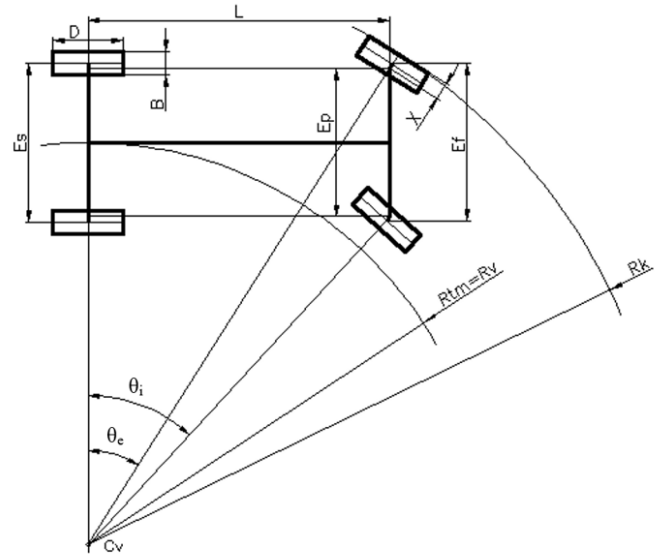


Figure 2. Scheme for calculating the kerb-to-kerb turning radius according to the median turning radius

The ADAMS Car program defines the turning radius of the vehicle, denoted in Figure 2 with $R_{tm}=R_v$, as the distance measured from the center of the turn to the longitudinal axis of the vehicle.

The technical documentation of motor vehicles specifies the minimum turning radius kerb-to-kerb, denoted in Figure 2 with R_k .

Between the two turning radius a relationship can be determined in relation to other design parameters. According to Figure 2, the following equations can be written:

$$\cos \theta_e = \frac{R_{tm} + \frac{E_p}{2}}{R_k - X} \quad (3)$$

$$X \cong \frac{E_f - E_p + B}{2} \quad (4)$$

where E_f represents the front track of the car, E_p is the distance between left and right spherical joints, B is the tire width, and X is the distance from the spherical joint axis to the outer circle of the turn. From relations (3) and (4) we have the kerb-to-kerb turning radius, R_k , given by the relation:

$$R_k = \frac{R_{tm} + \frac{E_p}{2} + \left(\frac{E_f - E_p + B}{2} \right) \cdot \cos \theta_e}{\cos \theta_e} = \frac{R_{tm} + \frac{E_p}{2}}{\cos \theta_e} + \frac{E_f - E_p + B}{2} \quad (5)$$

From eq. (1) the angle θ_e can be written as:

$$\theta_e = \arctg \frac{L}{R_{tm} + 0,5E_p} \quad (6)$$

Substituting the relation (6) in relation (5) results the expression of the kerb-to-kerb turning radius R_k , given by the relation:

$$R_k = \frac{R_{tm} + \frac{E_p}{2}}{\cos \left(\arctg \frac{L}{R_{tm} + 0,5E_p} \right)} + \frac{E_f - E_p + B}{2} \quad (7)$$

In order to determine the kerb-to-kerb turning radius, R_k , the corresponding values for the studied vehicle (BMW 328i) were used in eq. (7) and the median turning radius was obtained using ADAMS Car's steering analysis result. The values of these parameters are: $E_p=1384$ mm, $E_f=1472$ mm, $B=205$ mm, $R_{tm}=R_v=3692.24$ mm, $L=2725$ mm. With these values, the kerb-to-kerb turning radius is $R_k=5308.6$ mm.

3. VIRTUAL MODEL OF THE STEERING AND FRONT SUSPENSION SYSTEMS

The virtual model of the steering and of the front suspension systems for the studied compact car has been made using ADAMS Car software.

Starting with default templates of the MacPherson suspension and a rack-pinion steering system, both templates were modified to comply with the geometry of the real car, accordingly (figure 3).

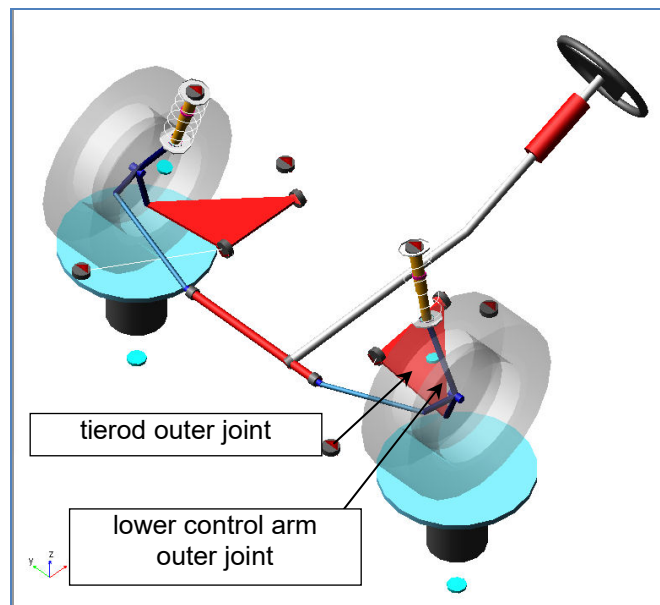


Figure 3. Virtual model of the steering and front suspension systems

The suspension parameters and some vehicle's characteristics such as wheel base, sprung mass, mass center height, tires dimensions, the wheels' mass were also set with corresponding values. This model is referred in this paper as "ini"-model. A steering analysis was made with a steering wheel rotation lock-to-lock of 3.4 rotations [12], and the variation of the Ackerman error and the turn radius were plotted (see Figure 4 for "ini"-model). The maximum value of Ackerman error was 3.99 deg. for the left wheel when the car is turning to the right and the left wheel is the outside wheel. Because of the symmetry of the steering linkage the results of the steering analysis were plotted for the left wheel only. The minimum median turn radius, R_{tm} , as shown in Figure 2, can be depicted from Figure 5 and its value was 3692.24 mm, corresponding with a turn radius kern-to-kern of 5308.6 mm (10617.2 mm turn diameter), calculated with eq. (7). The turn circle can be found in dedicated technical websites [12] with a value of 10500 mm. This is a variation of 1.12% which validate the virtual model.

4. DESIGN OPTIMIZATION

The aim of the design optimization was to find an optimal design solution of the steering system in order to minimize the Ackerman error and the turning radius of the vehicle so these were chosen as the objective functions of the optimization problem. The design variables were the X, Y and Z coordinates of the outer joints of the tie rod and of the lower control arm, see Figure 3. For each design variables a variation of ± 20 mm from nominal position were defined as domain constraints.

The design optimization of the initial model of the steering and front suspension systems has been made using ADAMS Insight with ADAMS Car. Adams Insight generates a design matrix according to specifications of the design type and the Box Behnken design was used with three levels [11].

The Box Behnken design needed a total number of 54 trials. The investigation strategy (method) for creating the design matrix was chosen the response surface method. This method fits polynomials to the results of the trials of the experiments. The polynomials were chosen to have a quadratic form.

5. THE RESULTS

After running all 54 trials, the optimal values of the design variables were found and the initial model was modified accordingly. This new model was named "opt"-model. A new steering analysis was made for this optimal model, and the results are presented in Figure 4 and Figure 5.

The Ackerman error had a maximum value of 3.99 deg. for the "ini"-model and this value was decreased to a maximum value of 2.28 deg. for the "opt"-model, which is 42.86% less (Figure 4).

In Figure 4, the maximum value of the Ackerman error is obtained for the end-lock position of the steering wheel to the right (-612 deg.) when the left wheel is the outer wheel of the turn.

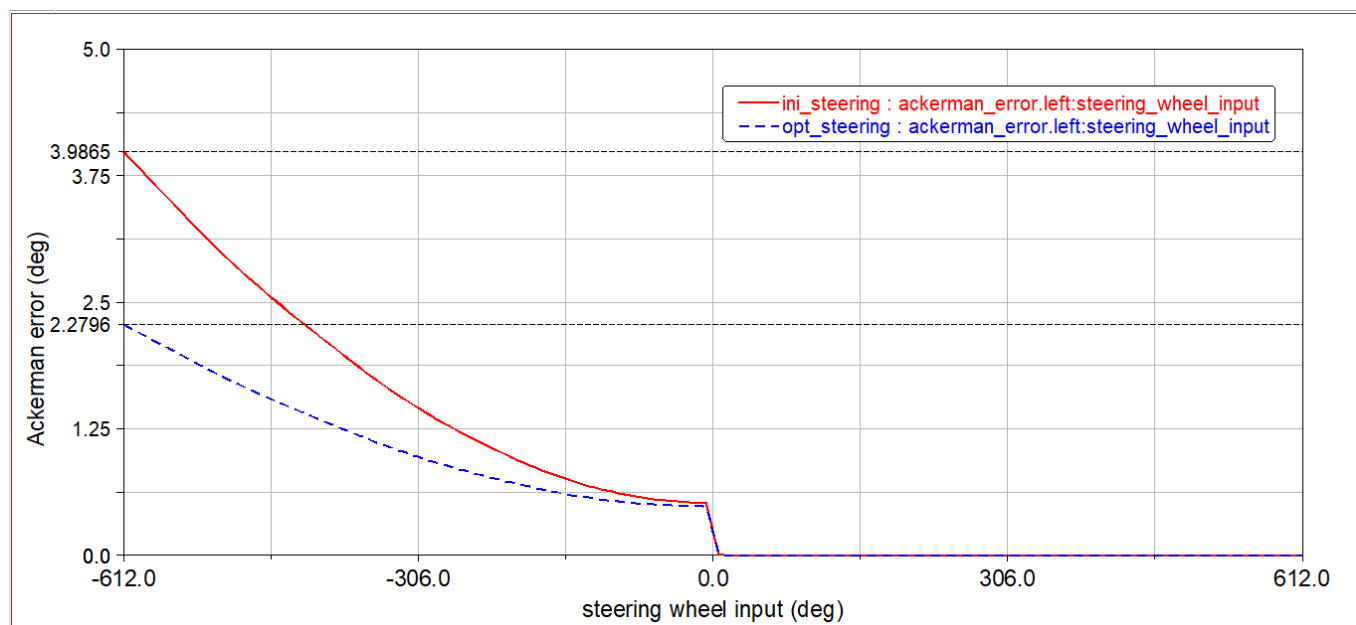


Figure 4. Ackerman error variation for the left wheel for initial and optimal models.

The variation of the median turning radius for both initial and optimal models is represented in Figure 5 for the left wheel, when the steering wheel is rotated from lock-to-lock positions. The maximum value of the median turn radius corresponds to the straight position of the steering wheel, and its value should be infinite. The minimum value of the median turning radius for the initial model was about 3692.2 mm for the right end-lock position of the steering wheel. This value was reduced to 3236.6 mm for the optimal model, which is a reduction with 12.34% of the median turn radius (which is R_{tm} in Figure 2). The optimal value of median turn radius corresponds to a value of the kerb-to-kerb turning radius of 4927.7 mm, using eq. (7) (turning circle of 9855.3 mm). This optimal value is lower than the one from initial model with 6.14%.

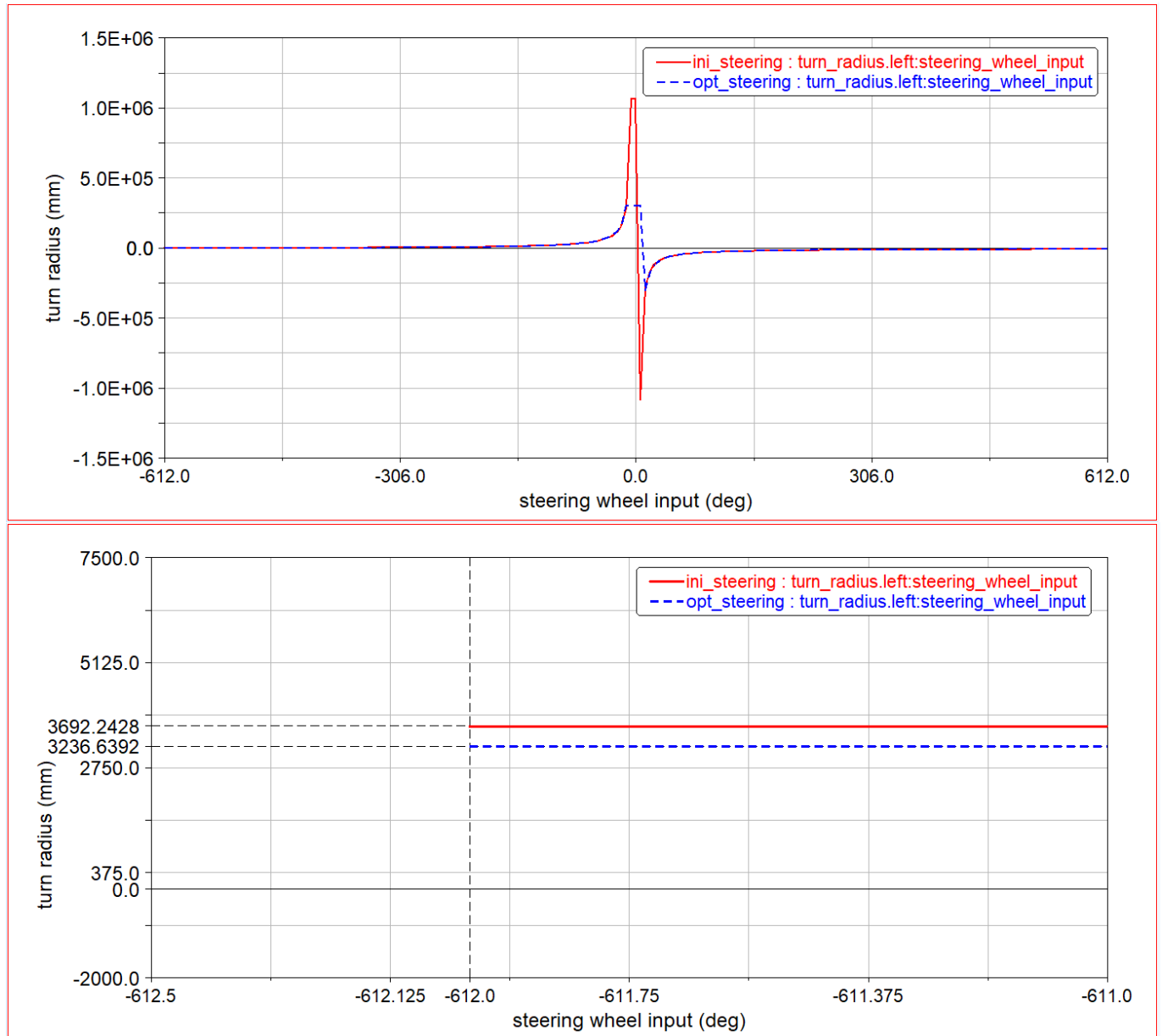


Figure 5. Variation of the median turn radius (R_{tm}); up: from lock-to-lock position of the steering wheel; down: detail for the right end-lock position of the steering wheel (-612 deg.)

5. CONCLUSION

Using a commercial software like ADAMS Car, the design engineers may evaluate the behavior of a vehicle even from design stage.

For a compact class vehicle, the steering system and the front suspension system were measured and a virtual model was built using ADAMS Car.

Running a steering analysis for this initial model, the variation of Ackerman error and the variation of the median turning radius were plotted.

The design optimization of the steering system involved the three coordinates of the spherical outer joints of the lower control arm and the tie rod as design variables and the optimal values of them lead to the optimal model.

The Ackerman error was reduced with 42.86% and the kerb-to-kerb turning radius was also reduced with 6.14% (approx. 0.65 m).

Reducing the Ackerman error for a steering system the tire wear may be reduced as the side slippage of the steered wheels is reduced during cornering.

For urban passenger cars, a reduced kerb-to-kerb turning radius leads to a greater maneuverability of the car especially in parking maneuvers.

REFERENCES

1. Zhou, B., Li, D., Yang, F.: *Optimization design of steering linkage in independent suspension based on genetic algorithm*, Proc. of Computer-Aided Industrial Design & Conceptual Design, Wenzhou, China (2009) 45-48
2. Slesongsom, S., Bureerat, S.: *Multiobjective optimization of a steering linkage*. In: *Journal Of Mechanical Science And Technology*, Volume 30, Issue 8, Pages 3681-3691, DOI 10.1007/s12206-016-0730-4, aug. 2016
3. Felzien, M. L., Cronin, D. L.: *Steering error optimization of the McPherson strut automotive front suspension*, Mechanism and Machine Theory, 20 (1985) 17-26
4. Guntur, R.R.: *Minimizing the steering error of an ackermann linkage*. In: *Arabian Journal For Science And Engineering*, Volume 16, Issue 1, Pages 45-52, JAN 1991
5. Simionescu, P. A., Smith, M. R.: *Initial estimates in the design of rack-and-pinion steering linkages*, Journal of Mechanical Design, 122 (2000) 194-200
6. Simionescu, P.A., Beale, D.: *Optimum synthesis of the four-bar function generator in its symmetric embodiment: the Ackermann steering linkage*. In: *Mechanism And Machine Theory*, Volume 37, Issue 12, Pages 1487-1504, Article Number PII S0094-114X(02)00071-X, DOI: 10.1016/S0094-114X(02)00071-X, dec. 2002
7. Stoicescu, A.P.: *On the optimization of an ackermann steering linkage*. In: UPB Scientific Bulletin, Series D: Mechanical Engineering, Vol. 75, Issue 4, P. 59-70, Bucharest (2013)
8. Zarak, C. E., Townsend, M. A.: *Optimal design of rack-and-pinion steering linkages*, Journal of Mechanical Design, 105 (1983) 220-226
9. Zhao, J.-S., Liu, X., Feng, Z.-J., Dai, J.S.: *Design of an Ackermann-type steering mechanism*. In: *Proceedings of the Institution of Mechanical Engineers, Part C: Journal of Mechanical Engineering Science*, Volume 227, Issue 11, Pages 2549-2562, China (November 2013).
10. Untaru, M., Stoicescu, A., Tabacu, I., Poțincu, Gh., Pereș, Gh.: *Dinamica autovehiculelor pe roți*, Editura Didactică și Pedagogică, Bucharest (1981)
11. ADAMS Car 2017.1- User Manual
12. <http://www.carinf.com/en/ac40410490.html>, last accesed 2018/04/10

RoJAE Romanian Journal of Automotive Engineering

AIMS AND SCOPE

The Romanian Journal of Automotive Engineering has as its main objective the publication and dissemination of original research in all fields of „Automotive Technology, Science and Engineering”. It fosters thus the exchange of ideas among researchers in different parts of the world and also among researchers who emphasize different aspects regarding the basis and applications of the field.

Standing as it does at the cross-roads of Physics, Chemistry, Mechanics, Engineering Design and Materials Sciences, automotive engineering is experiencing considerable growth as a result of recent technological advances. The Romanian Journal of Automotive Engineering, by providing an international medium of communication, is encouraging this growth and is encompassing all aspects of the field from thermal engineering, flow analysis, structural analysis, modal analysis, control, vehicular electronics, mechatronics, electro-mechanical engineering, optimum design methods, ITS, and recycling. Interest extends from the basic science to technology applications with analytical, experimental and numerical studies.

The emphasis is placed on contribution that appears to be of permanent interest to research workers and engineers in the field. If furthering knowledge in the area of principal concern of the Journal, papers of primary interest to the innovative disciplines of „Automotive Technology, Science and Engineering” may be published.

No length limitations for contributions are set, but only concisely written papers are published. Brief articles are considered on the basis of technical merit. Discussions of previously published papers are welcome.

Notes for contributors

Authors should submit an electronic file of their contribution to the **Production office**: www.siar.ro. All the papers will be reviewed and assessed by a series of independent referees.

Copyright

A copyright transfer form will be send to the author. All authors must sign the "Transfer of Copyright" agreement before the article can be published.

Upon acceptance of an article by the journal, the author(s) will be asked to transfer copyright of the article to the publisher. The transfer will ensure the widest possible dissemination of information. This Journal and the individual contributions contained in it are protected by the copyright of the SIAR, and the following terms and conditions apply to their use:

Photocopying

Single Photocopies of single articles may be made for personal use as allowed by international copyright laws. Permission of the publisher and payment of a fee is required for all other photocopying including multiple or systematic copying, copying for institutions that wish to make photocopies for non-profit educational classroom use.

Derivative Works

Subscribers may reproduce table of contents or prepare lists of article including abstracts for internal circulation within their institutions. Permission of the publisher is required for resale or distribution outside the institution.

Permission of publisher is required for all other derivative works, including compilations and translations.

Electronic Storage

Permission of the publisher is required to store electronically and material contained in this journal, including any article or part of article. Contact the publisher at the address indicated.

Except as outlined above, no part of this publication may be reproduced, stored in a retrieval system or transmitted in any form or by any means, electronic, mechanical, photocopying, recording or otherwise, without prior written permission of the publisher.

Notice

No responsibility is assumed by the publisher for any injury and or damage to persons or property as a matter of products liability; negligence or otherwise, or from any use or operation of any methods, products, instructions or ideas contained in the material herein. Although all advertising material is expected to conform to ethical (medical) standards, inclusion in this publication does not constitute a guarantee or endorsement of the quality or value of such product or of the claims made of it by its manufacturer.

The logo for SIAR (The Society of Automotive Engineers of Romania) is displayed in a stylized, bold, blue font.

The Journal of the Society of Automotive Engineers of Romania

www.ro-jae.ro www.siar.ro

ISSN 2457 – 5275 (Online, English)

ISSN 1842 – 4074 (Print, Online, Romanian)

RoJAE Romanian Journal of Automotive Engineering

ISSN 2457 – 5275 (Online, English)
ISSN 1842 – 4074 (Print, Online, Romanian)

The Scientific Journal of SIAR A Short History

The engineering of vehicles represents the engine of the global development of the economy.

SIAR tracks the progress of the automotive engineering in Romania by: the development of automotive engineering, the development of technologies, and road transport services; supporting the work of the haulers, supporting the technical inspection and of the garage; encouraging young people to have a career in the automotive engineering and road haulage; stimulation and coordination of activities that promote an environment that is suitable for continuous education and improving of knowledge of the engineers; active exchange of ideas and experience, in particular for students, master students, PhD students, and young engineers, and dissemination of knowledge in the field of automotive engineering; cooperation with other technical and scientific organizations, employers' and socio-professional associations through organization of joint actions, of mutual interest.

By the accession to FISITA (International Federation of Automotive Engineering Societies) since its establishment, SIAR has been involved in achieving an overall professional community that is homogeneous in competence and performance, interactive, dynamic, and competitive at the same time, oriented towards a balanced and friendly relationship between people and the environment; this action will be constituted as a challenge worthy of effort and recognition.

The insurance of a favorable framework for the initiation and the development of cooperation of the specialists in this field of activity allows for an efficient and easy exchange of information, specific knowledge and experience; it supports the cooperation between universities and between research centers and industry; it speeds up the process of implementing the new technologies, it simplifies the identification of training and specialization needs of the personnel involved in the engineering of motor vehicles, transport, and road safety.

In order to succeed, ever since its founding, SIAR has considered that the stress should be put on the production and distribution, at national and international level, of a publication of scientific quality.

Under these circumstances, the development of the scientific magazine of SIAR had the following evolution:

1. RIA – Revista inginerilor de automobile (in English: *Journal of Automotive Engineers*)

ISSN 1222 – 5142

Period of publication: 1990 – 2000

Frequency: Quarterly

Total number of issues: 30

Format: print, Romanian

Electronic publication on: www.ro-jae.ro

Type: Open Access

The above constitutes series nr. 1 of SIAR scientific magazine.

2. Ingineria automobilului (in English: *Automotive Engineering*)

ISSN 1842 – 4074

Period of publication: as of 2006

Frequency: Quarterly

Total number of issues: 51

(including the June 2019 issue)

Format: print and online, Romanian

Electronic publication on: www.ingineria-automobilului.ro

Type: Open Access

The above constitutes series nr. 2 of SIAR scientific magazine (Romanian version).

3. Ingineria automobilului (in English: *Automotive Engineering*)

ISSN 2284 – 5690

Period of publication: 2011 – 2014

Frequency: Quarterly

Total number of issues: 16

(including the December 2014 issue)

Format: online, English

Electronic publication on: www.ingineria-automobilului.ro

Type: Open Access

The above constitutes series nr. 3 of SIAR scientific magazine (English version).

4. Romanian Journal of Automotive Engineering

ISSN 2457 – 5275

Period of publication: from 2015

Frequency: Quarterly

Total number of issues: 18 (June 2019)

Format: online, English

Electronic publication on: www.ro-jae.ro

Type: Open Access

The above constitutes series nr. 4 of SIAR scientific magazine (English version).

Summary – on June 30, 2019

Total of series:

4

Total years of publication:

25 (11: 1990 – 2000; 14: 2006 – 2019)

Publication frequency:

Quarterly

Total issues published:

81 (Romanian), out of which, the last 34 were also published in English



SIAR

Societatea Inginerilor de Automobile din România
Society of Automotive Engineers of Romania
www.siar.ro
www.ro-jae.ro